https://doi.org/10.5194/egusphere-2025-5385
Preprint. Discussion started: 18 November 2025

Biochemical Characteristics of the Sea Surface Microlayer in the Central Baltic Sea and Potential Signatures of Cyanobacterial Blooms

Josefine Karnatz[1], Theresa Barthelmeß[1], Bita Sabbaghzadeh[2], Anja Engel[1,3]

[1]Marine Biogeochemistry, GEOMAR Helmholtz Centre for Ocean Research Kiel, Kiel, 24148, Germany
[2]Leibniz Institute for Baltic Sea Research, Warnemünde, Germany
[3]Christian Albrechts University of Kiel, Germany

Correspondence to: Josefine Karnatz (jkarnatz@geomar.de)

Abstract. The sea surface microlayer (SML) forms the <1mm thin ocean's boundary with the atmosphere and plays a critical role in mediating air–sea gas exchange and biogeochemical cycling. However, the biological processes shaping its molecular composition remain insufficiently understood. During a research cruise in the central Baltic Sea (Eastern Gotland Basin), we investigated how phytoplankton, including cyanobacteria, influence the biomolecular composition of the SML. Although no major bloom was detected, distinct shifts in phytoplankton composition were observed, leading to pronounced differences in biomolecular characteristics between the SML and underlying water (ULW), and between conditions characterized by high and low cyanobacteria abundance. While SML enrichment patterns and carbohydrate concentrations were comparable to those previously reported for the Western Baltic Sea, concentrations of total amino acids (TAA) and surfactants were substantially higher, suggesting enhanced production by cyanobacteria. Distinct molecular signatures were associated with different phytoplankton size classes. During periods of high abundance of small phytoplankton (HPA<20 µm; *Synechococcus*-dominated), the SML was characterized by elevated surfactant and total combined carbohydrate (TCCHO) concentrations. Furthermore, *Synechococcus sp.* co-varied with the non-protein amino acid γ-aminobutyric acid (GABA), particularly under HPA<20 µm conditions. This suggests that the production of surface-active organic matter may be linked to *Synechococcus sp.* In contrast, under high abundance of large phytoplankton (HPA>20µm; filamentous and colonial cyanobacteria), total amino acids (TAA), particulate amino acids (PAA>20µm), and particulate combined carbohydrates (PCCHO>20µm) were enhanced in the ULW, mirroring POC>20µm and cyanobacterial biomass patterns. The significant correlation between phytoplankton >20µm biomass and POC>20µm suggests that the particulate organic carbon pool was largely cyanobacteria-derived, even in the absence of a distinct bloom. Together, our results imply that phytoplankton size structure and taxonomy exert distinct biomolecular imprints on SML chemistry in the Central Baltic Sea. The contrasting roles of filamentous/colonial cyanobacteria (proteinaceous signatures) and *Synechococcus* (carbohydrate/surface-activity imprint) imply community-dependent modulation of surface activity and, indicate that changes in biodiversity may potentially impact air–sea gas exchange in the ocean.

https://doi.org/10.5194/egusphere-2025-5385
Preprint. Discussion started: 18 November 2025

1 Introduction

The sea surface microlayer (SML) forms the ocean's uppermost boundary, directly linking the hydrosphere and atmosphere. The SML covers up to 70% of Earth's surface (Wurl et al., 2017), and plays a pivotal role in global biogeochemical processes (Engel et al., 2017)despite its narrow vertical extent, typically ranging from 50 to 1000 µm (Zhang et al., 2003; Cunliffe et al., 2013). Positioned at the air–sea interface, the SML modulates the exchange of climate-relevant gases such as dimethyl sulphide (DMS), carbon dioxide (CO_2), and methane (CH_4) (Engel et al., 2017), thereby influencing key climate processes (Wurl et al., 2017). These biogeochemical interactions are largely governed by the enrichment of surface-active biomolecules derived from biological production and organic matter cycling (Cunliffe et al., 2013; Thornton, 2014; Engel and Galgani, 2016; Engel et al., 2017; Wurl et al., 2017).

Phytoplankton are the primary source of dissolved organic matter (DOM) in the ocean and contribute substantially to the organic enrichment of the SML. Through exudation, cell breakage, and lysis, phytoplankton release a wide range of organic compounds, including lipids, proteins, amino acids, and carbohydrates which shape the biochemical composition and dynamics of the SML (Parrish, 1998; Thornton, 2014; Galgani and Engel, 2016; Engel et al., 2018). Transparent exopolymer particles (TEP) and Coomassie stainable particles (CSP) constitute particulate fractions of extracellular polymeric substances (EPS) released by phyto- and bacterioplankton, forming polymeric organic matrices that vary in size, composition, and structure. These particles contribute to the gelatinous and cohesive nature of the SML (Cunliffe and Murrell, 2009; Dreshchinskii and Engel, 2017).

Among the organic compounds accumulating in the SML are surface-active agents (surfactants). The accumulation of surface-active organic matter affects gas transfer velocity (k) by altering its hydrodynamic properties. Surfactants can reduce k by forming viscous films that suppress small scale turbulence and dampen capillary waves (Frew et al., 2004; Jenkinson et al., 2018). A large-scale oceanic in the Atlantic demonstrated that surfactant enrichment can significantly reduce CO_2 exchange rates, even under moderate to high wind conditions (Sabbaghzadeh et al., 2017). Thus, air–sea gas transfer is highly sensitive to the presence of surfactants at the ocean's surface (Schmidt and Schneider, 2011; Pereira et al., 2018). Surfactant accumulation is particularly pronounced in regions of elevated primary production and has been associated with phytoplankton blooms, grazing, and bacterial degradation (Zutic et al., 1981; Kujawinski et al., 2002; Tsai and Liu, 2003; Satpute et al., 2010).

Phytoplankton blooms further shape the microbial community inhabiting the SML, the bacterioneuston, through the release of organic substrates that sustain heterotrophic metabolism (Cunliffe et al., 2013; Taylor et al., 2014). During microbial degradation of phytoplankton exudates, high-molecular-weight polymers can be converted into smaller, more amphiphilic molecules. Additionally, bacterioneuston taxa can produce biosurfactants such as glycolipids and lipopeptides that directly lower surface tension (Abraham et al., 1998; Cunliffe et al., 2013; Kurata et al., 2016; Engel et al., 2017). While mesocosm and incubation experiments have linked phytoplankton blooms to enhanced surfactant concentrations and the accumulation of fresh organic material in the SML (Zutic et al., 1981; Galgani and Engel, 2013), field observations remain limited by coarse

https://doi.org/10.5194/egusphere-2025-5385
Preprint. Discussion started: 18 November 2025

temporal and spatial resolution. As a result, the coupling between phytoplankton bloom dynamics and the release of surface-active biomolecules in natural systems is still poorly constrained. Despite the recognized influence of phytoplankton production on organic matter composition in the SML (Wurl et al., 2011; Galgani and Engel, 2013), little is known about how specific phytoplankton species alter the molecular and biogeochemical composition of the SML under natural conditions.

The semi-enclosed Baltic Sea represents an ideal system to explore these coupled dynamics of phytoplankton blooms, the release of surface-active biomolecules, and the resulting changes in the molecular composition of the SML due to its pronounced spatial and seasonal variability in nutrient inputs, phytoplankton productivity, and community composition (Murray et al., 2019). The Central Baltic Sea is particularly susceptible to extensive summer blooms of filamentous cyanobacteria, promoted by warming waters, enhanced stratification, and low nitrogen-to-phosphorus ratios resulting from eutrophication and widespread anoxia (Hajdu et al., 2007; Thornton, 2018). Climate-driven changes in stratification are expected to further intensify the occurrence and persistence of such blooms (Paerl and Paul, 2012). Filamentous cyanobacteria in the Baltic Sea are diazotrophic, i.e. capable of fixing atmospheric N_2, and dominate the summer phytoplankton biomass when dissolved nitrogen is depleted (Kahru and Elmgren, 2014; Munkes et al., 2021). The bloom-forming taxa, *Nodularia spumigena*, *Aphanizomenon sp*., and *Dolichospermum spp*., form extensive surface accumulations across the Central Baltic Sea, including the Eastern Gotland Basin, typically peaking between July and August (Wasmund, 1997; Kahru and Elmgren, 2014; Karlson et al., 2015, 2022). Their filamentous morphology is sustained by specific filament-forming proteins (Springstein et al., 2020), and protein-rich EPS, including CSP, have been observed in *Nodularia spumigena* cultures (Endres et al., 2013; Zhi et al., 2023), suggesting a potentially significant contribution to extracellular amino acid pools.

Biochemical studies in the Baltic Sea have shown that the SML is enriched in amino compounds and carbohydrates relative to the underlying water (Van Pinxteren et al., 2012). In mesocosm experiments, proteinaceous gels (CSP) abundance was five times higher than that of carbohydrate-rich gels in the SML (Galgani and Engel, 2013). Time-series data from the coastal Boknis Eck station in the Western Baltic Sea further demonstrated recurring enrichment of amino acids and CSP in the SML during spring (Dreshchinskii and Engel, 2017). Phytoplankton-derived biopolymers, including amino-acid- and carbohydrate-like components, are thus potential key contributors to surface activity in this region, and are characterized by short turnover times and diel variability typical of fresh phytoplankton exudates (Van Pinxteren et al., 2012; Barthelmeß and Engel, 2022). Laboratory and field studies further suggest that cyanobacteria produce EPS and glycolipids with pronounced surface activity, facilitating microlayer film formation and altering interfacial properties (De Philippis and Vincenzini, 1998). The release of such compounds can result in visible surface slicks, which locally warm the upper sub-millimeter ocean skin and modify near-surface physical processes (Wurl et al., 2018). Under low-wind conditions in the Baltic Sea, the SML rapidly reorganizes into slick-like, polymer- and particle-rich states, consistent with enhanced surface activity during bloom periods (Stolle et al., 2010). During such periods, particulate organic carbon can contribute up to 55% of the surfactant pool (Gašparović and Ćosović, 2003). Seasonal records further indicate that surfactant concentrations peak during summer months following the spring bloom and reflecting intensified solar radiation (Laß et al., 2013).

https://doi.org/10.5194/egusphere-2025-5385
Preprint. Discussion started: 18 November 2025

Taken together, cyanobacteria represent major producers of extracellular organic matter, including amino acids, carbohydrates, lipids, and amphiphilic metabolites, that may substantially influence the surfactant pool in the Baltic Sea. This study aims to address the current knowledge gap regarding the role of cyanobacteria in shaping the biomolecular composition of the SML. Using a Neuston catamaran and an underlying water net, we collected phytoplankton (>20 µm) and accompanying samples from the uppermost surface and 1 m depth in the central Baltic Sea. SML samples for characterizing the organic matter and phytoplankton <20µm were collected by applying specialized samplers, such as the glass plate (Harvey and Burzell, 1972) and the Garrett Screen (Garrett, 1965). To evaluate the influence of cyanobacteria, including filamentous species, we assessed the variability of key biomolecular classes in relation to high and low phytoplankton abundance across size fractions. Our overarching goal was to determine how cyanobacteria modulate the biochemical composition of the SML, with implications for gas exchange processes as inferred from surfactant analysis.

2 Methods

2.1 Research area

Samples were collected in July (30.06. – 19.07. 2022) during the cruise EMB295 with the *RV Elisabeth Mann Borgese* in the Central Baltic Sea. The cruise was part of the project "Central Baltic Sea Air Sea Exchange Experiment" (CenBASE). All sampling stations were located in the Eastern Gotland Basin, between 19.1° and 20.2°E and 57.10° and 57.30°N (Fig. 1). Two stations were sampled daily, one in the morning at 6 am and one in the afternoon at 6 pm local time for a total of 15 stations (Table A1). During the cruise, surface waters (3m) had a salinity of 7.26 ± 0.10 PSU and a temperature of 18.86 ± 0.22 °C.

https://doi.org/10.5194/egusphere-2025-5385
Preprint. Discussion started: 18 November 2025

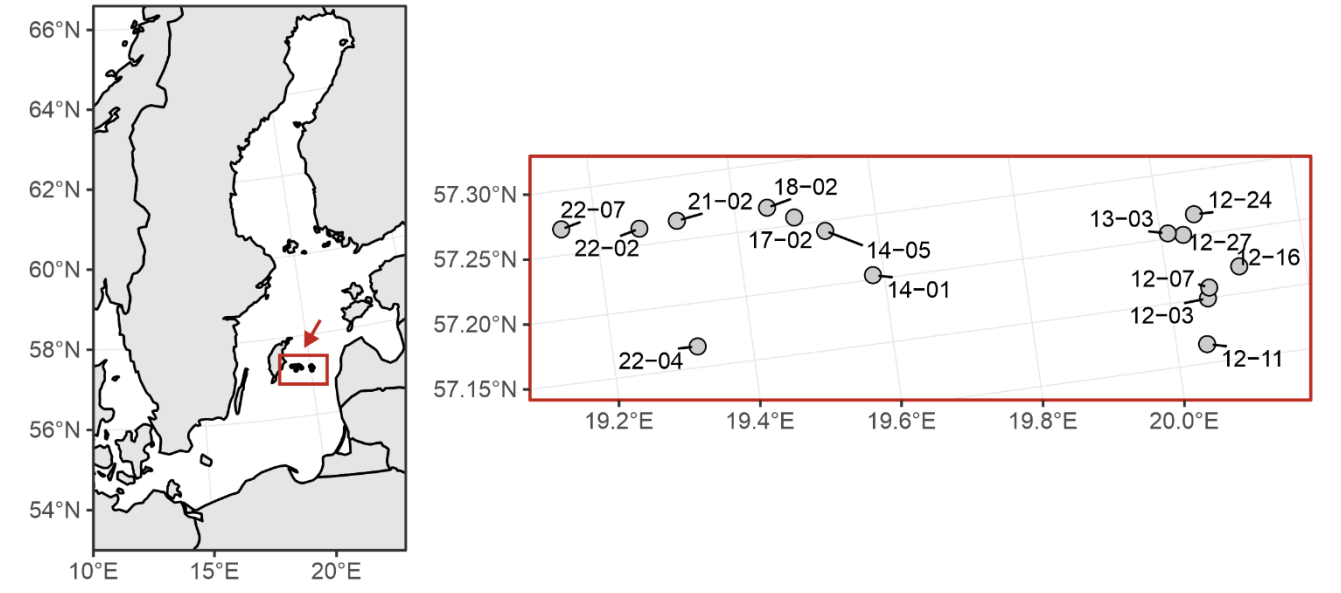

Figure 1: The study area east of Gotland in the Central Baltic Sea is indicated by the red inset (left). The enlarged view of the Eastern Gotland Basin shows the sampling stations, labelled with their station IDs, from the EMB295 cruise (right).

2.2 Sampling

At each station, seawater and particles (>20µm) were sampled. Particles >20µm were collected from the surface using a Neuston catamaran (Fig. S1) and from ~1m depth using a ULW net (Fig. S2). Seawater was sampled from the SML using a glass plate or a Garret Screen and from the ULW by a manually operated 2L Niskin bottle.

The Neuston catamaran, equipped with a 20µm mesh-size net attached, was towed at 3 knots on starboard, allowing for the sampling of the upper ~20 cm of the surface. Towing time for the Neuston catamaran was between ~5 min and ~17 min, equivalent to 594 and 15950 L seawater. In order to determine the amount of water that flowed through the net, a flowmeter (Hydro-Bios) was attached below the net opening, which was used to calculate the amount of water based on its rotations as follows:

$$V = N \times 0.3A \times 1000 \quad (1)$$

with V (L) being the sampled water volume, N the number of revolutions, and A the area of the net opening (m^2). The ULW reference depth was sampled with an ULW net with a mesh size of 20µm and attached to a V-fin and towed with 1.5 knt from starboard at approximately 1 m depth. Towing time was between ~5 min and ~14min, equivalent to 1636 and 12204 L seawater. The net opening area (A) was 0.0225 m^2 for the catamaran and 0.045 m^2 for the ULW net. During periods of strong wave action, the flow meter in the catamaran net opening occasionally emerged above the water surface, interrupting revolutions and yielding low or irregular counts. Consequently, sampled volumes calculated from N come with uncertainty. Before hauling

https://doi.org/10.5194/egusphere-2025-5385
Preprint. Discussion started: 18 November 2025

in the Neuston catamaran and ULW net, the nets were rinsed with seawater from the outside, so that the entire content of the net was rinsed into the net sock. Once the net was on deck, the samples were rinsed with filtered seawater into a beaker. Due to the high biomass retained in the nets, the samples were diluted with filtered seawater, for which water was collected from 5m depth and filtered through 3µm and 0.2µm pore size. Samples were diluted in different ratios from 2:1 to 1:2 (vol:vol) depending on the thickness of the net catch and gently swirled before subsampling to ensure a homogeneous sample. Consequently, net samples included the particulate fraction >20µm and the added filtered seawater. Net samples were stored at 4°C between subsampling.

Seawater sampling was conducted from a working boat positioned ~500 m upwind of the research vessel to minimize contamination and ensure an undisturbed surface. The SML was sampled with the glass plate (Cunliffe & Wurl, 2014; Harvey and Burzell, 1972) and collected into sample-rinsed amber borosilicate glass bottles (250 mL). Before sampling, the glass plate and frame were conditioned by sequential rinses with ambient seawater and a small volume of SML sample. Samples were kept shaded in an isolated box and processed within ≤2 h. For cleaning, the glass plate and bottles were soaked in 10% HCl and thoroughly rinsed with Milli-Q water. The wiper and its frame were flushed with freshwater and then rinsed with Milli-Q. When working boat operations were not possible due to bad weather, the SML was sampled using a Garrett screen (Garrett, 1965) from the bow of the vessel as described in Barthelmeß et al. (2021). ULW was collected at 1m using a manually operated Niskin bottle (2L) and filled into a borosilicate bottle (250 mL).

In the following, Neuston catamaran and ULW net sample depth are referred to as “Surface” and “ULW-Net”, respectively. The term “SML” refers to the sampled depth collected with the glass plate or Garrett screen, and “ULW” denotes the reference depth sampled with the manual Niskin Bottle.

2.3 Microphytoplankton microscopy

Microphytoplankton (>20µm) were subsampled from net catches. After dilution of the net-tow samples as described above, 200 mL aliquots were transferred to amber glass bottles, preserved with 2 mL acidic Lugol’s solution, and stored at 4 °C until processing. For analysis, samples were diluted (1:15 or 1:30) with water of the corresponding salinity, transferred to sedimentation chambers (Hydro-Bios), and left overnight to allow particle settling. Phytoplankton community analysis included taxonomic identification (species composition), microscopic enumeration of abundance (Utermöhl, 1958; DIN EN 15972:2011-11), and biovolume estimation based on measurements of a representative number of cells per taxon (DIN EN 16695:2015-12). Microscopy was performed with a ZEISS Axiovert 25 inverted microscope at 100x, 200x, and 400x magnification. Where possible, organisms were identified to species level, otherwise, they were assigned to genus level or higher taxonomic groups. For microphytoplankton samples only the 8 most dominant phytoplankton species were identified: *Aphanizomenon sp.*, *Aphanocapsa sp.*, *Nodularia spumigena*, *Cylindrotheca closterium*, *Pseudo-nitzschia delicatissima*, *Chaetoceros sp.*, *Dinophysis sp.*, and *Diplopsalis* (group). For each sample, at least 400 individuals were enumerated, and approximately 20 individuals per taxon were measured for their visible dimensions. For biovolume estimation, each taxon was assigned an appropriate geometric body, and volume was calculated from the measured dimensions. When certain dimensions

https://doi.org/10.5194/egusphere-2025-5385
Preprint. Discussion started: 18 November 2025

could not be measured (e.g., due to cell orientation in the chamber), standard correction factors were applied in accordance with DIN EN 16695:2015-12. Abundance was calculated accounting for the dilution factor and reported as cells per sample volume. Biomass was calculated based on biovolume and species-specific carbon content per cell. Throughout this study, microphytoplankton determined by microscopy are referred to as "Phytoplankton >20µm".

2.4 Flow cytometry

Samples for flow cytometry were taken from SML and ULW. Duplicates of 1.7 mL were preserved with 85 µL glutaraldehyde (GDA), and stored at −80 °C until later analysis. Phytoplankton and bacterial cells were quantified using a flow cytometer (Becton, Dickinson and Company FACSCalibur; software - BD Biosciences CellQuest Pro), calibrated with yellow-green latex beads (0.5 and 1 µm in diameter). Autotrophic cells were detected based on their autofluorescence (Marie et al., 1997), classified according to size in picophytoplankton (<2µm) and nanophytoplankton (2–20 µm), and further differentiated by their characteristic pigments into chlorophyll *a*- and phycoerythrin-rich pico- and nanophytoplankton after Engel & Galgani (2016) and Zäncker et al. (2017). Picophytoplankton with phycoerythrin were affiliated to *Synechococcus* (Marie et al., 2010). We estimated the biomass of *Synechococcus sp.* based on cell counts. Reported estimates of *Synechococcus* cellular carbon biomass range from approximately 0.1 to 1.5 pg C cell^{-1} (Moisan et al., 2010). Here, we used an average carbon biomass of 0.3 pg C cell^{-1} based on Buitenhuis et al. (2012). In the following, phytoplankton cells determined by flow cytometry are referred to as "Phytoplankton <20µm".

2.5 Chlorophyll *a* (Chl *a*)

Chlorophyll *a* (Chl *a*) samples were taken in duplicates from the Niskin bottles at 1m depth (ULW). For each sample, 500 mL seawater were filtered onto a GF/F filter (Whatman, 25mm) flash-frozen in liquid nitrogen and stored at –80°C. Analyses were performed within one year of sample collection. Samples were acidified and measured with a fluorometer from Turner Designs (Turner TD 10-AU005) with an excitation at 450 nm and an emission of 670 nm.

2.6 Organic matter analysis

For determination of total organic carbon (TOC) from SML and ULW, 20 mL were filled into pre-combusted (8 hours at 500°C) glass ampules and acidified by adding 20 µL of 30% hydrochloric acid (HCl, Suprapure, Sigma-Aldrich). After acidification, the samples were flame-sealed and stored at 4°C until analysed with a TOC analyser (TOC-VCSH, Shimadzu) following Engel and Galgani (2016). TOC analysis was validated daily using deep seawater reference (DSR) material from the Consensus Reference Materials Project of RSMAS (University of Miami), yielding values within the certified range of 42–45 µmol C L^{-1}. Two internal standards with DOC similar to samples were daily prepared using potassium hydrogen phthalate (Merck 109017). TOC concentrations in each sample were determined from 5 to 8 injections, with precision (<4%) estimated as the standard deviation divided by the mean. Total nitrogen (TN) was determined in parallel with TOC using the TNM-1 detector on the Shimadzu analyser. Nitrogen is combusted and transformed to NOx, which chemi-luminesces when mixed

https://doi.org/10.5194/egusphere-2025-5385
Preprint. Discussion started: 18 November 2025

with ozone and was detected using a photomultiplier (Dickson et al., 2007). The instrument was calibrated every 8–10 days using standard solutions (0, 500, 1000, 1500, 2500, and 5000 µg C L^{-1}) prepared from a potassium hydrogen phthalate standard (Merck 109017). On each measurement day, ultrapure water determined the instrument blank. The detection limit of TOC was 1µM.

For POC>20µm, duplicate 20 mL samples of the surface and ULW-Net samples, including the particulate fraction and filtered seawater, were filled into ampules. From each ampoule, two aliquots (0.5–2.0 mL) were filtered onto pre-combusted (8 hours at 500°C) GF/F filters (Whatman, 25 mm) at low constant vacuum (<0.2 mbar), and the filtrate was collected in pre-acid-washed (HCl) Falcon tubes and stored at 4°C. POC filters were stored at –20°C until later analysis for less than a year. For the measurement, filters were wrapped in tin cups and measured using an Euro EA elemental analyser calibrated with an acetanilide standard after Sharp (1974). Filters with ultrapure water were measured as lab blank per run (<10 µg C per filter). During storage, particulate carbon may have dissolved. Therefore, the filtrate was measured in the same way as the TOC samples (see above). After the separated analyses, the carbon concentrations of the filtrate and filters were combined and reported as POC>20µm. Values were corrected by subtracting the TOC concentration of pre-filtered seawater (ranged between 341.07–457.15 µM) used to rinse the sample out of the net.

On board, samples for total combined carbohydrates >1 kDa (TCCHO) and total amino acids (TAA) were collected from both SML and ULW sample into 20 mL and 4 mL pre-combusted glass vials and stored at –20°C. Particulate fractions of combined carbohydrates (PCCHO >20µm) and amino acids (PAA >20µm) were determined from net samples and treated identically as the total fraction, i.e., filled into pre-combusted glass vials of the same respective volumes and stored at −20 °C. TCCHO and PCCHO>20µm were determined by high-performance anion-exchange chromatography coupled to pulsed amperometric detection (HPAEC-PAD) with a DIONEX ion chromatography system (ICS 6000) (Engel and Händel, 2011). The following neutral sugars were quantified: glucose, mannose and xylose, galactose, arabinose, fucose and rhamnose, the acidic sugars galacturonic acid and glucuronic acid and the amino sugars galactosamine and glucosamine.

TAA and PAA>20µm were determined using a high-performance liquid chromatography (HPLC) system following Dittmar et al., (2009) and Lindroth & Mopper, (2025). The following thirteen amino acids were quantified: aspartic acid, glutamic acid, serine, glycine, threonine, arginine, alanine, tyrosine, valine, isoleucine, phenylalanine, and leucine.

The detection limit for combined carbohydrates and amino acids was 5−10 nM and ~1 nM, respectively (Dittmar et al., 2009.; Engel & Händel, 2011). Amino acid and carbohydrate concentrations are expressed in their carbon-equivalent in µM C, and the corresponding concentrations in µM.

2.7 Surfactants

For surface activity analysis, triplicates of 18 mL SML and ULW samples were transferred by a syringe into pre–acid-washed (HCl) and pre-combusted (8h, 500°C) 20 mL glass vials, and immediately stored at −20 °C. One of three replicate samples was analysed. Sample were measured within 12 months after collection using phase-sensitive alternating current voltammetry

https://doi.org/10.5194/egusphere-2025-5385
Preprint. Discussion started: 18 November 2025

(797 VA Computrace polarograph Metrohm, Switzerland), following the method initially introduced by Cosović & Vojvodić (1982). This technique is based on the discharge of an electrochemical double layer formed at the polar–non-polar interface of a hanging mercury drop electrode (Scholz, 2015), which interacts with surfactants present in the sample. The resulting changes in capacitive current, relative to a pure electrolyte blank, were used to quantify environmental surfactants. Prior to measurement, the samples ionic strength was standardized by adding an appropriate volume of a 3M sodium chloride (NaCl) solution. Samples were measured in glass vials at room temperature. Measurements were conducted with a 60 s deposition time and a voltage sweep ranging from −0.6 V to −1 V. To prevent contamination, all measuring vials were pre-cleaned with 10% HCl, rinsed with Milli-Q water, and combusted at 500°C overnight. Calibration was performed using the artificial, non-ionic surfactant Triton X-100 (TX-100, Sigma-Aldrich, Germany, molecular weight: 625 g mol^{-1}).

2.8 Data handling

Statistical analysis was executed in RStudio (Version 2025.05.0). Data analysis comprised the calculation of mean (M) and standard deviation (SD), and all reported values follow the format M ± SD unless indicated otherwise. The median was used as a threshold to divide the dataset into two groups, ensuring an equal number of samples in each group and allowing for balanced statistical comparison. For characterizing the SML, enrichment factors (EFs) were calculated by dividing the concentration in the SML by the corresponding ULW:

$$\mathbf{EF} = \frac{[\boldsymbol{C}_{\mathbf{SML}}]}{[\boldsymbol{C}_{\mathbf{ULW}}]} \quad (2)$$

For statistical comparison of the biomass, abundance, and depth pairs, if both groups had $n \geq 3$ and passed a Shapiro–Wilk normality test ($p > 0.05$ in each group), a two-sample Welch's t-test was used; otherwise, a Wilcoxon rank-sum test. We considered that null hypotheses testing and correlations were significant at $p < 0.05$.

For correlations, relative abundances were used. Parameters with only two data points (*Diplopsalis* and *Dinophysis sp.*) were excluded from the correlation. Correlations between taxon-specific phytoplankton biomass and relative concentrations of PCCHO, TCCHO, PAA and TAA were tested using Spearman's rank correlation (ρ). Analyses were conducted separately for the SML/surface and ULW/ULW-Net by subsetting the dataset by depth. To facilitate structure-revealing visualization, carbohydrates and amino acids were ordered by their similarity of correlation patterns with biomass in the SML and ULW. Significances were encoded in the correlation matrices as *, **, and *** for $p < 0.05$, $p < 0.01$, and $p < 0.001$, respectively.

3. Results

3.1 Phytoplankton distribution and composition

To examine whether filamentous cyanobacteria influence the biomolecular composition of seawater in the SML and ULW, we compared stations with varying phytoplankton abundances, and differentiated between >20µm and <20µm size classes.

https://doi.org/10.5194/egusphere-2025-5385
Preprint. Discussion started: 18 November 2025

Figure 2 shows the station-specific abundances of phytoplankton >20µm and <20µm for sampled depths, estimated by microscopy and flow cytometry, respectively. The dashed lines represent the median values calculated from ULW-Net and ULW samples, i.e. 300 x 10^3 cells mL^{-1} for phytoplankton >20µm (incl. *Aphanizomenon sp.*, *Aphanocapsa sp.*, *Nodularia spumigena*, *Aphanizomenon sp*., *Cylindrotheca closterium*, *Pseudo-nitzschia delicatissima*, *Chaetoceros sp*., *Dinophysis sp*., and *Diplopsalis* (group)) and 53 × 10^3 cells mL^{-1} for phytoplankton <20µm (incl. Chl *a*- and phycoerythrin-rich pico- and nanoplankton), respectively. Stations with ULW concentrations above the respective medians were classified as "high," while those below were classified as "low." Accordingly, phytoplankton >20µm abundance was grouped into high (HPA>20µm) and low (LPA<20µm) categories (Fig. 2b), and phytoplankton <20µm abundance into high (HPA<20µm) and low (LPA<20µm) categories (Fig. 2c). A summary of this classification is provided in Table A2. Overall, the spatial patterns of phytoplankton abundance and Chl *a* reflected pronounced variability across the stations (Fig. 2).

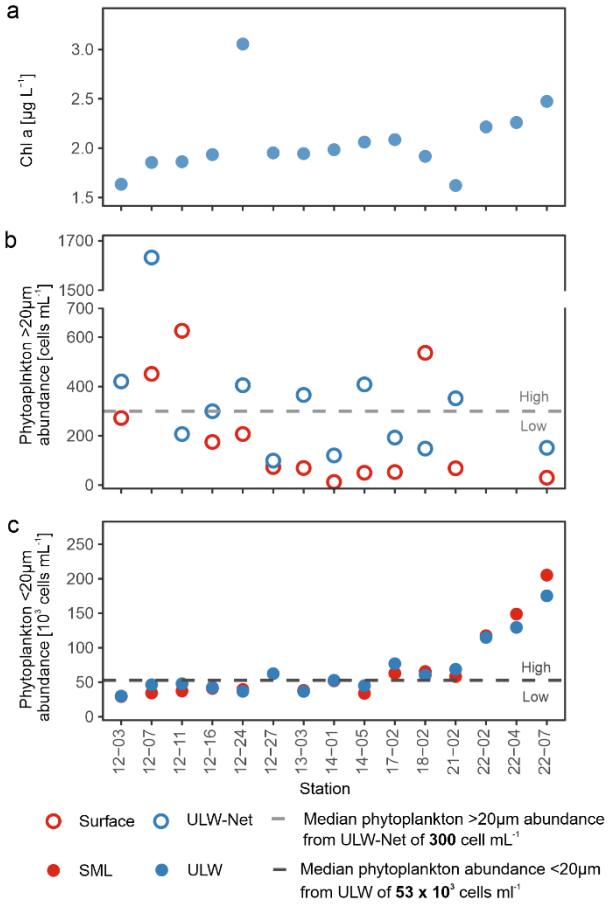

Figure 2: Chlorophyll *a* (Chl *a*) concentrations (a) in the underlying water (ULW), (b) phytoplankton abundance >20µm in surface net samples and ULW-Net samples and (c) phytoplankton <20µm abundance for SML and ULW across stations sampled during EMB 295. The dashed horizontal light- and dark-grey lines mark the median abundances according to the size classes. Samples were grouped into low phytoplankton >20µm abundance (LPA>20µm) or low phytoplankton <20µm abundance (LPA<20µm) if below

https://doi.org/10.5194/egusphere-2025-5385
Preprint. Discussion started: 18 November 2025

the median values in the ULW and high phytoplankton >20µm abundance (HPA>20µm) or high phytoplankton <20µm abundance (HPA<20µm) if above. Station order corresponds to temporal sequence of sampling conducted during the cruise.

Chl *a* concentrations in the ULW ranged from 1.60 to 3.05 µg L^{-1} (2.06 ± 0.35 µg L^{-1}), showing a gradual increase towards stations 22–07, except for station 12-24 and stations 18–02, and 21-02 (Fig. 2a). Phytoplankton >20µm abundance ranged between 12.7 and 1658 cells mL^{-1} with an overall mean of 287 ± 327 cells mL^{-1} with one high value at station 12–07 (1658 cells mL^{-1}) (Fig. 2b). At station 22–02 and 22–04, weather conditions were too rough to deploy the Neuston catamaran and ULW net, thus no net samples could be taken. Abundances of phytoplankton <20µm (Fig. 2c) increased in both the SML and ULW from station 12–03 to 21–02, followed by a pronounced step increase towards station 22–07, where the maximum value (205 x 10^3 cells mL^{-1}) was recorded. In 10 out of 13 common stations, the abundances of phytoplankton >20µm were inversely related to those of the <20µm fraction, indicating that stations characterized by elevated abundances of >20µm phytoplankton generally showed reduced abundances of phytoplankton <20µm, and vice versa.

https://doi.org/10.5194/egusphere-2025-5385
Preprint. Discussion started: 18 November 2025

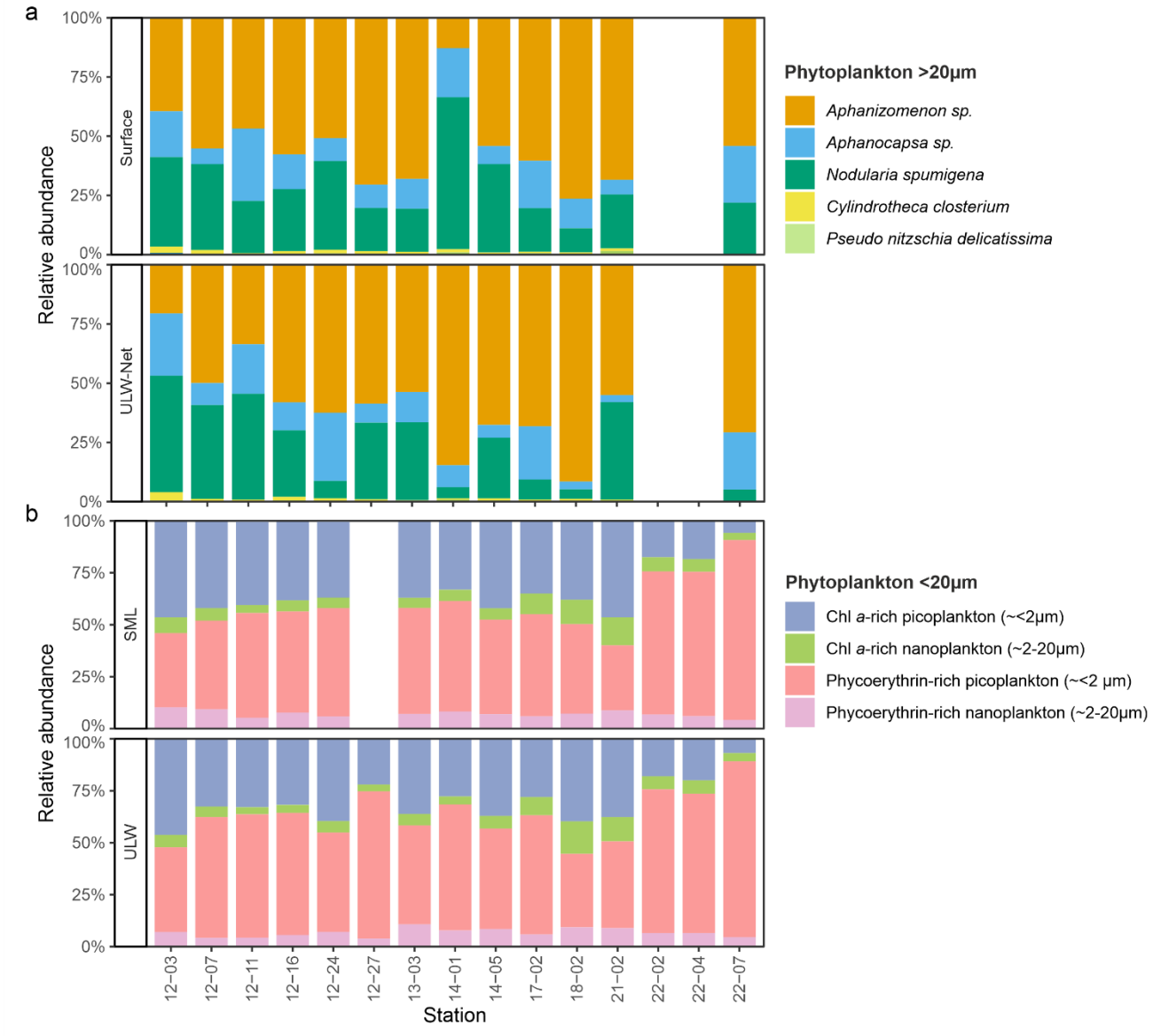

Figure 3: Stacked bar plot of the relative abundance for (a) dominant phytoplankton species (>20 µm) in surface and ULW-Net samples, and (b) the relative abundance of the four phytoplankton groups (<20µm) in SML and ULW samples. Colors for phytoplankton >20µm denote five of the eight identified phytoplankton taxa. Abundance of *Chaetoceros sp. Dinophysis sp.*, and *Diplopsalis* (group) were <1% and are not shown.

Across the stations, the >20µm phytoplankton community was strongly cyanobacteria-dominated in both surface and ULW-Net samples (Fig. 3a). *Aphanizomenon sp*. was the dominant species at almost all stations and in both layers and accounted for a mean abundance of 158 ± 169 cells mL^{-1}. Secondary contributions came from *Nodularia spumigena* (84 ± 130 cells mL^{-1}), followed by *Aphanocapsa sp*. (41 ± 49 cells mL^{-1}), which were consistently present but more variable among stations. Diatoms

https://doi.org/10.5194/egusphere-2025-5385
Preprint. Discussion started: 18 November 2025

were a minor component of the >20µm phytoplankton community. *Cylindrotheca closterium* (3.3 ± 4.5 cells mL^{-1}) and *Pseudo-nitzschia delicatissima* (1.1 ± 0.8 cells mL^{-1}) were typically present at low percentages (<2%). Overall, variability in relative species abundance among stations was moderate, and the dominance of filamentous cyanobacteria persisted across the section and depths. Relative abundances for *Chaetoceros sp*., *Dinophysis sp*. and *Diplopsalis* (group) were <2% and are thus not visible in Fig. 3. Higher resolution of the relative abundance <4% can be found in the supplementary material (Fig. S3).

Picoplankton containing the pigment phycoerythrin (*Synechococcus*) were most abundant (42 ± 41 x 10^3 cells mL^{-1}) representing at almost all stations more than 50% of the total community by number at almost all stations, i.e. SML-phytoplankton <20µm: 69 ± 52 x 10^3 cells mL^{-1} and ULW-phytoplankton <20µm: 68 ± 41 x 10^3 cells mL^{-1}, followed by picophytoplankton containing Chl *a* (18 ± 5.0 x 10^3 cells mL^{-1}) (Fig. 3b). During stations 22–02, 22–04, and 22–07, phycoerythrin-rich picoplankton abundance increased in the SML and ULW up to 178 x 10^3 cells mL^{-1} and 148 x 10^3 cells mL^{-1}, respectively, and made up more than 80% of the phytoplankton <20µm community by number. Nanophytoplankton varied little between stations and depth. Chl *a*-rich nanoplankton showed mean values about 4.3–4.5 ± 3.0 10^3 cells mL^{-1} in the SML and ULW. Phycoerythrin-rich nanoplankton varied about 4.5 ± 2.4 x 10^3 cells mL^{-1} in the SML and 4.4 ± 2.3 x 10^3 cells mL^{-1} in the ULW. Overall, *Aphanizomenon* sp. exhibited the highest phytoplankton >20µm abundance, followed by *Nodularia spumigena* and *Aphanocapsa* sp.. Phytoplankton <20µm abundances were approximately three orders of magnitude higher than those of phytoplankton >20µm. Microscopic analysis enabled biomass estimation of phytoplankton >20µm. Pronounced differences in the biomass of dominant >20µm phytoplankton taxa between surface and ULW samples were observed during both LPA>20µm and HPA>20µm periods, as shown in Figure 4. In addition, calculated *Synechococcus sp.* (phycoerythrin-rich picoplankton) biomass (see section 2.4) was included for same conditions to enable comparison with the >20µm phytoplankton fraction.

https://doi.org/10.5194/egusphere-2025-5385
Preprint. Discussion started: 18 November 2025

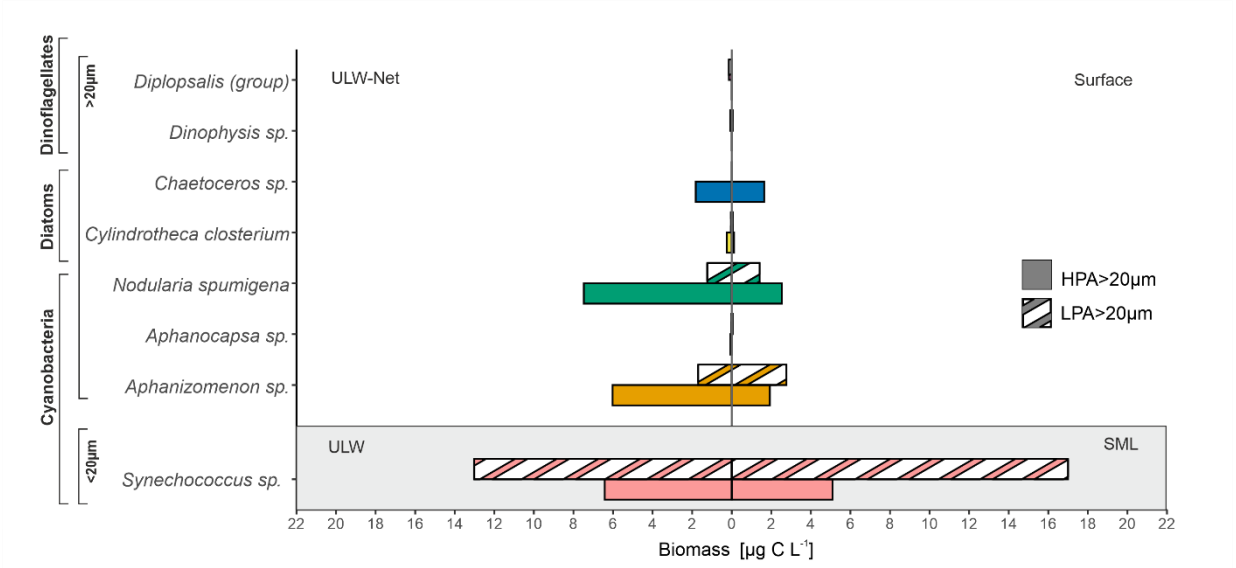

Figure 4: Mean biomass (µg C L⁻¹) of dominant phytoplankton >20µm taxa and *Synechococcus sp*. (<20 µm) in surface and ULW-Net samples, as well as *Synechococcus sp.* in SML and ULW samples for *Synechococcus sp*. Data are differentiated by phytoplankton abundance level (solid bars = HPA>20µm, High Phytoplankton >20 µm Abundance; hatched bars = LPA>20µm, Low Phytoplankton >20µm Abundance). Bars represent biomass for each taxon, with colors indicating species identity. *Pseudo-nitzschia delicatissima* was excluded from the figure due to its negligible biomass contribution (<0.01 µg C L⁻¹).

In general, phytoplankton biomass >20µm was higher in the ULW-Net with an overall mean of 8.98 ± 10.93 µg C L^{-1} compared to the surface biomass of 4.59 ± 4.32 µg C L^{-1}. The highest biomass contributions within phytoplankton species >20µm were from *Aphanizomenon sp*. and *Nodularia spumigena* ranging from 0.05 to 16.04 µg C L^{-1} and 0.16 to 26.55 µg C L^{-1}, respectively. *Nodularia spumigena* showed the highest biomass in the ULW at HPA>20µm (7.48 ± 8.72 µg C L^{-1}). *Aphanizomenon sp.* occurred in both layers with generally greater values in the ULW-Net at HPA>20µm (6.0 ± 4.7 µg C L^{-1}). *Cylindrotheca closterium* and *Chaetoceros sp*. occurred at HPA>20µm only with < 0.2 µg C L^{-1}). Other taxa, including *Aphanocapsa sp*., *Dinophysis sp*., and *Diplopsalis* (group), made up less than 0.1 µg C L^{-1}.

Synechococcus sp. exhibited higher biomass than the >20µm phytoplankton taxa, with a mean value of 12.63 ± 12.18 µg C L^{-1}, showing no significant difference between SML and ULW samples. Under HPA>20µm (which corresponds mostly with LPA<20µm conditions), *Synechococcus sp.* biomass was considerably lower (5.76 ± 1.58 µg C L^{-1}) compared to LPA>20µm conditions (which corresponds to HPA<20µm conditions), during which it increased to 16.41 ± 16.35 µg C L^{-1}. In summary, the phytoplankton community was characterized either by dominance of filamentous cyanobacteria or *Synechococcus sp*..

3.2 Biomolecular concentrations are shaped by phytoplankton

The concentrations of the biochemical parameters were grouped into HPA/LPA >20µm and HPA/LPA<20µm, in order to elucidate potential influences of the different phytoplankton classes. An overview of all parameters is provided in the

https://doi.org/10.5194/egusphere-2025-5385
Preprint. Discussion started: 18 November 2025

Supplement (Fig. S5 & S6). In the following, we focus on those parameters that exhibit the most pronounced differences (Fig. 5 and Fig. 6).

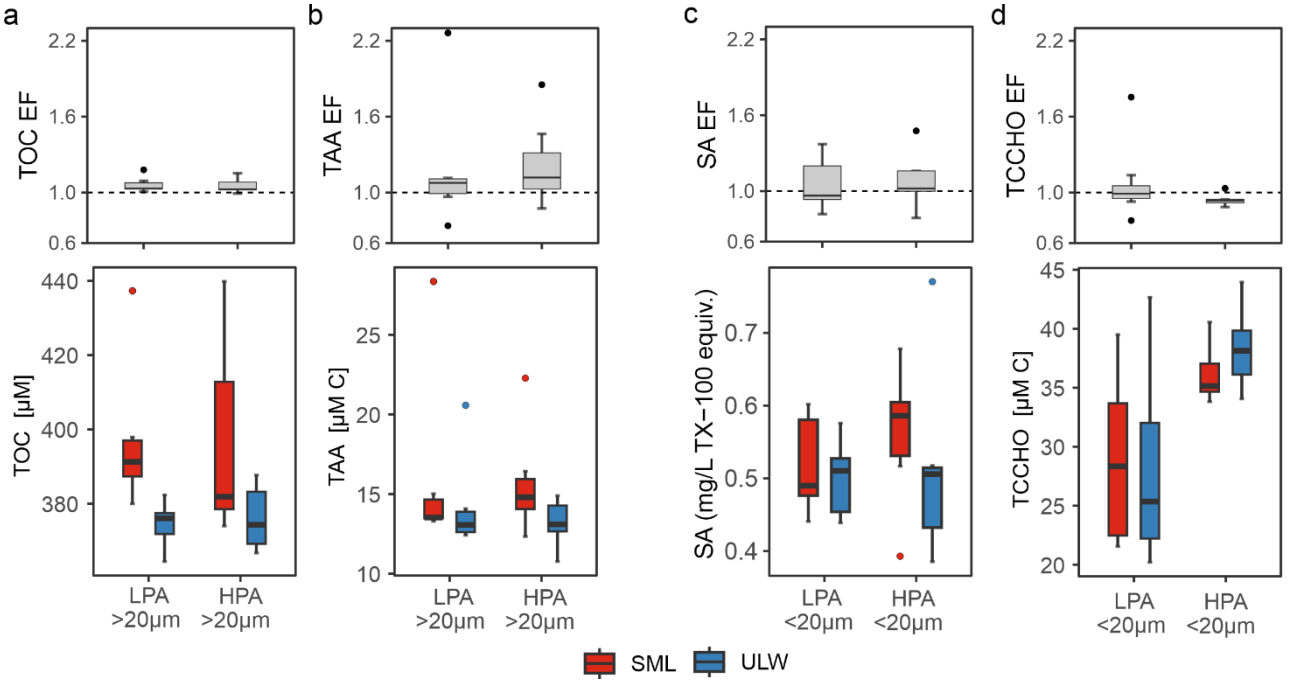

Figure 5: Concentration differences during low phytoplankton >20µm abundance (LPA>20µm) and high phytoplankton >20µm abundance (HPA>20µm) for SML and ULW for (a) total organic carbon (TOC), and (b) total amino acids (TAA). surfactants (c) and total combined carbohydrates (TCCHO) (d) were differentiated for high and low phytoplankton <20µm abundance (HPA<20µm and LPA<20µm) . Enrichment factors (EF) for each parameter are shown for the respective abundance groups.

TOC concentrations (Fig. 5a) showed a clear enrichment in the SML during LPA>20µm conditions, with significantly higher values in the SML (398 ± 23 µM) compared to the underlying water layer (ULW; 375 ± 6 µM, p = 0.006). Despite the increase, EFs were close to 1 across stations (1.1 ± 0.1). Under HPA>20µm conditions, TOC concentrations did not differ significantly between the two depths. TAA concentrations (Fig. 5b) increased slightly from 14.29 ± 3.14 µM C (≙ 3.30 ± 0.72 µM) in the ULW to 16.20 ± 5.99 µM C (≙ 3.85 ± 1.52 µM) in the SML under LPA>20µm conditions. In the SML, TAA showed a higher median concentration during HPA>20µm (14.8 µM C) than during LPA>20µm (13.59 µM C), although mean values did not differ. This tendency was more pronounced in the <20µm size fraction (Fig. S6a), where TAA concentrations were slightly higher under LPA<20µm conditions (14.86 ± 2.80 µM C ≙ 3.46 ± 0.69 µM) than under HPA<20µm conditions (14.06 ± 4.27 µM C ≙ 3.32 ± 1.08 µM). When samples were pooled across categories (i.e., not distinguished by HPA/LPA), TAA concentrations differed significantly between depths (SML: 15.43 ± 4.34 µM C ≙ 3.65 ± 1.10 µM; ULW: 13.55 ± 2.21 µM C ≙ 3.14 ± 0.50 µM; p = 0.076), resulting in an average EF of 1.2 ± 0.4 (median = 1.1). During HPA<20µm conditions, surfactant concentrations (Fig. 5c) were elevated in the SML (0.56 ± 0.09 mg L^{-1} TX-100 equiv.) relative to the ULW (0.52 ± 0.14 mg L^{-1} TX-100 equiv.), corresponding to an EF of 1.1 ± 0.2 (median = 1.1). In contrast, surfactant EFs were lower under LPA<20µm conditions (1.1 ± 0.2; median = 1.0). This pattern is further supported by the >20µm size fraction (Fig. S5c),

https://doi.org/10.5194/egusphere-2025-5385
Preprint. Discussion started: 18 November 2025

where during LPA>20µm higher surfactant concentrations were detected in the SML (0.56 ± 0.11 mg L^{-1} TX-100 equiv.) compared to the ULW (0.45 ± 0.06 mg L^{-1} TX-100 equiv.) and average EF of 1.2 ± 0.2 (median: 1.3). TCCHO concentrations (Fig. 5d) were significantly elevated during HPA<20 µm conditions (37.21 ± 3.0 µM C ≙ 6.38 ± 0.50 µM) compared to LPA<20 µm (28.36 ± 7.18 µM C ≙ 4.85 ± 1.23 µM, p = 0.007). Depth-related differences in TCCHO remained insignificant. Station-specific enrichment factors are presented in the Supplement (Fig. S7).

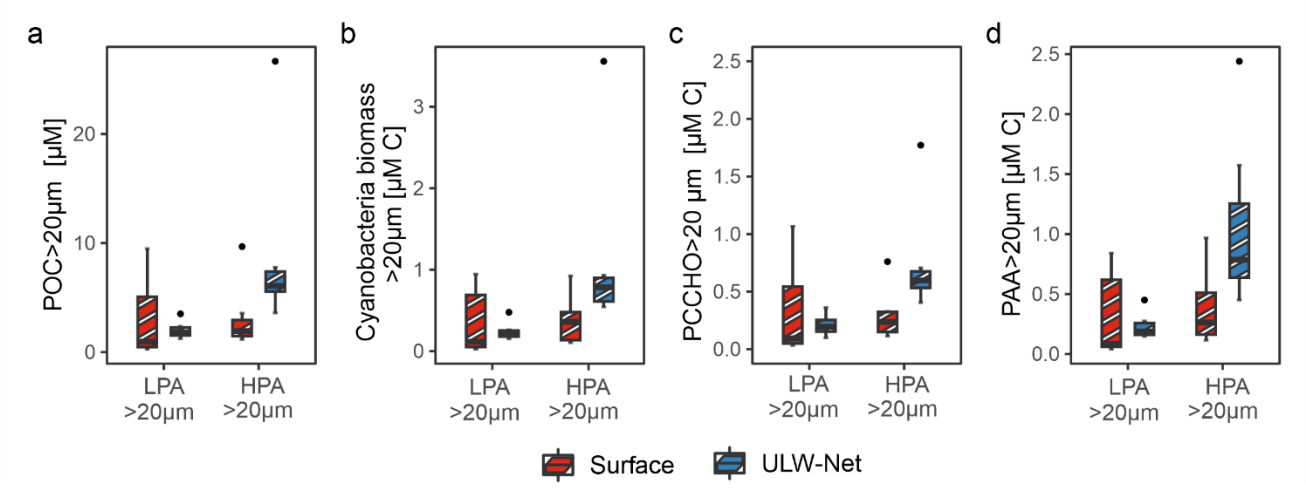

Figure 6: Concentration differences during low phytoplankton >20µm (LPA>20µM) and high phytoplankton >20µm abundance (HPA>20µM) conditions for (a) particulate organic carbon (POC) >20µm, (b) cyanobacteria biomass >20µm, (c) particulate combined carbohydrates >20µm (PCCHO>20µm), and (d) particulate amino acids >20µm (PAA>20µm) for surface (red, striped) and ULW-Net (blue, striped) samples.

During HPA>20µm conditions, POC>20µm concentrations differed significantly between depths, with markedly higher values in the ULW-Net (8.89 ± 7.95 µM) compared to the surface (3.09 ± 3.02 µM; p = 0.02). In contrast, depth-related differences were not evident under LPA>20µm conditions, where concentrations were lower in both the surface (3.07 ± 3.92 µM) and ULW-Net (2.04 ± 0.82 µM) compared to HPA>20µm.

Within the POC>20µm pool, phytoplankton contributed on average 12.7 ± 4.6% to the total POC>20µm, with the cyanobacteria dominating the assemblage (Fig. 6b). Their biomass reached 1.13 ± 1.08 µM C in the ULW-Net and was significantly reduced at the surface (0.37 ± 0.29 µM C; p = 0.01). Similar patterns were reflected in PCCHO>20µm (Fig. 6c), which showed elevated concentrations in the ULW-Net (0.74 ± 0.46 µM C ≙ 0.12 ± 0.08 µM) compared to the surface (0.29 ± 0.22 µM C ≙ 0.05 ± 0.04 µM; p = 0.02). These compounds represented 10.3 ± 2.3% of the POC>20µm pool and 1.3 ± 1.2% of TCCHO, contributing 1.7 ± 1.3% and 0.9 ± 0.9% under HPA>20µm and LPA>20µm conditions, respectively. A comparable trend was observed for PAA>20µm (Fig. 6d), which increased from 0.38 ± 0.32 µM C (≙ 0.08 ± 0.07 µM) at the surface to 1.07 ± 0.71 µM C (≙ 0.23 ± 0.16 µM) in the ULW-Net (p = 0.05). PAA>20µm contributed 12.9 ± 6.4% to the POC>20µm pool and 0.3–18.6% (3.8 ± 4.1%) to TAA, with relatively higher contributions during HPA>20µm (5.4 ± 4.8%) than LPA>20µm (1.9 ± 1.9%) conditions.

https://doi.org/10.5194/egusphere-2025-5385
Preprint. Discussion started: 18 November 2025

Overall, surfactants, and TOC tended to exhibit higher SML concentrations during LPA>20µm. TAA concentrations, however, were marginally higher during HPA>20µm conditions. Conversely, particulate fractions (PAA>20µm and PCCHO>20µm) reflected the expected enrichment of cyanobacterial biomass and POC>20µm in the ULW-Net under HPA>20µm conditions. Further, we found that phytoplankton >20µm biomass was significantly related to POC>20µm ($R^2 = 0.94$; $p < 0.001$) (Fig. S4) and accounted for 5.4 -28.5% (mean: 12.7%) of the POC pool, primarily driven by the contributions of *Nodularia spumigena* and *Aphanizomenon sp*..

3.3 Biomolecular composition of amino acids and carbohydrates

To highlight distinct differences in compound composition between the size classes, the relative molecular composition of amino acids and combined carbohydrates for the total and particulate (>20µm) fractions were compared (Fig. 7).

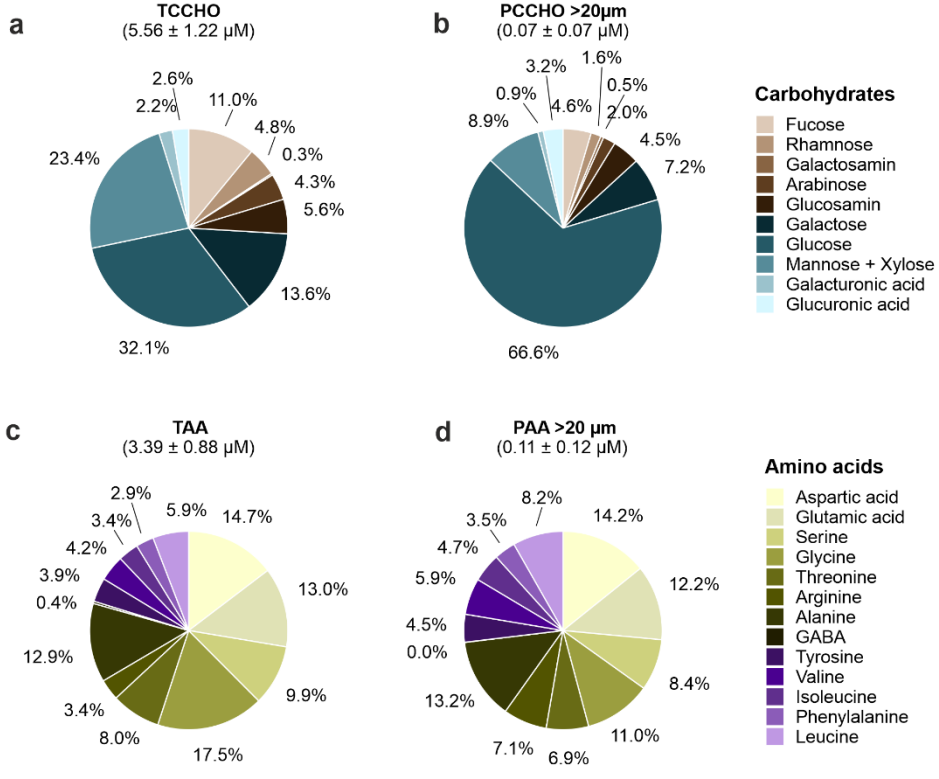

Figure 7: Composition of combined carbohydrates and amino acids in total and particulate pools. The pie charts summarize the relative contributions of individual compounds (a) to total combined carbohydrates (TCCHO), (b) particulate combined carbohydrates (PCCHO), (c) total amino acids (TAA), and (d) particulate amino acids (PAA). Slice labels give each mol% of the pool. Chart titles report the M ± SD concentration (µM) of the molecular concentrations of the corresponding pool across all samples.

A few key compounds strongly dominated carbohydrate composition, while several constituents contributed only marginally. TCCHO (5.6 ± 1.2 µM) was characterized by a predominance of glucose (32.1 mol%) and mannose & xylose (23.4 mol%), followed by galactose (13.6 mol%) and glucosamine (11.0 mol%). In the particulate pool (>20 µm) (0.06 ± 0.07 µM), glucose

https://doi.org/10.5194/egusphere-2025-5385
Preprint. Discussion started: 18 November 2025

dominance became even more pronounced, accounting for 66.6 mol%, while the contributions of mannose & xylose (8.9 mol%), galactose (7.2 mol%), and glucosamine (4.5 mol%) were comparatively smaller. An elevated fraction of glucuronic acid and galactosamine was also characteristic of the PCCHO pool in comparison to the TCCHO pool. Amino acid composition was characterized by a more diverse contribution of individual compounds. The total amino acid pool (TAA: 3.4 ± 0.8 µM) was mainly composed of glycine (17.5 mol%), aspartic acid (14.7 mol%), glutamic acid (13.0 mol%), and alanine (12.9 mol%). The particulate fraction (PAA>20 µm; 0.11 ± 0.12 µM) exhibited a comparable composition, dominated by aspartic acid (14.2 mol%), glutamic acid (12.2 mol%), alanine (13.2 mol%), and glycine (11.0 mol%). Shifts in relative proportions suggest subtle differences in the source of amino acids between fractions. Relative shifts in the contributions of GABA, arginine, leucine, phenylalanine, valine, and tyrosine were observed. While GABA was elevated in the TAA pool, the later amino acids were enriched within the particulate pool (Fig. 7d, mainly purple).

https://doi.org/10.5194/egusphere-2025-5385
Preprint. Discussion started: 18 November 2025

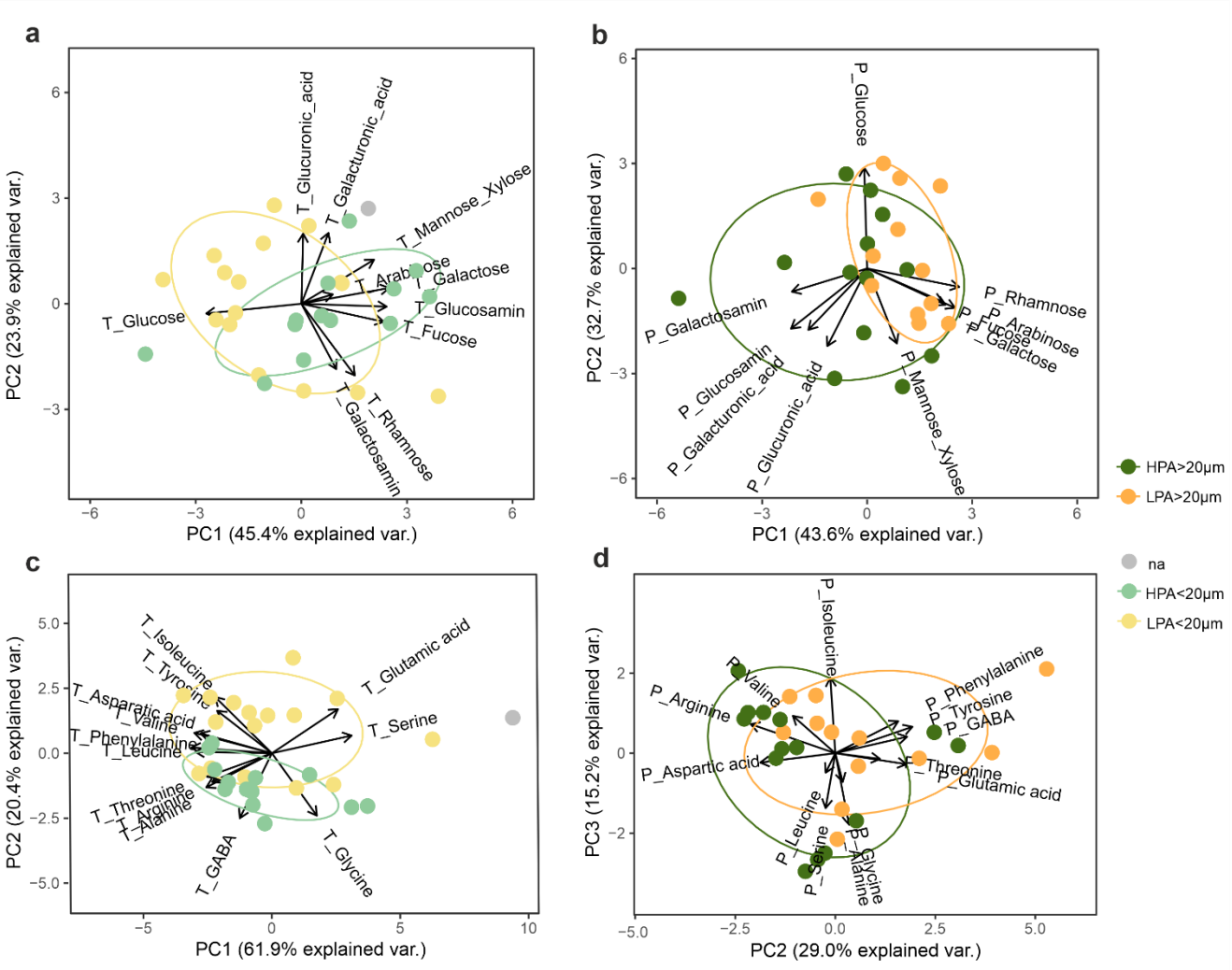

Figure 8: Principal component analysis (PCA) was conducted for both size classes. Biplots show (a) total combined carbohydrates (TCCHO), (b) particulate combined carbohydrates (PCCHO), (c) total amino acids (TAA), (d) and particulate amino acids (PAA). Scores are colored by HPA<20µm (light green), LPA<20µm (light yellow), HPA>20µm (dark green) and LPA>20µm (dark yellow). Arrows show variable loadings; axes are scaled to unit variance and annotated with percent variance explained. Stations for which no phytoplankton <20µm abundance data were available are annotated as 'na', preventing assignment to a specific abundance level.

Principal component analysis (PCA) revealed systematic compositional differences between low (LPA<20µm) and high (HPA<20µm) phytoplankton abundance (Fig. 8). For total combined carbohydrates (Fig. 8a), PC1 and PC2 explained 45.4% and 23.3% of the variance, respectively, and together accounted for 68.7% variation in the data. LPA<20µm was mainly characterized by the high contribution of total glucose, while HPA<20µm showed higher contributions of total galactose, glucosamin, fucose and mannose & xylose. For total amino acids (Fig. 8c), the PC1 explained 61.9% of the variance (PC2: 20.4%), while categories separated mainly along PC2. Positive PC2 loadings were driven by total glutamic acid, isoleucine and tyrosine, whereas negative PC2 loadings were associated with e.g. total GABA and glycine. The PC1 axis, explaining

https://doi.org/10.5194/egusphere-2025-5385
Preprint. Discussion started: 18 November 2025

most of the variance, was loosely related to a separation between ULW (negative values, e.g., phenylalanine, leucine, arginine, tyrosine) and the SML (positive values for glutamic acid, serine, glycine) (Fig. S8).

The compound-specific analysis of PCCHO and PAA > 20µm (Fig. 8b, d) revealed distinct compositional differences between HPA > 20µm and LPA > 20µm, primarily separating along PC1 (explained variance: 43.6%) and PC2 (explained variance: 29.0%), respectively. During HPA>20µm, PCCHO was characterized by elevated contributions of galactosamine, along with notable proportions of glucosamine, galacturonic acid, and glucuronic acid (Fig. 8b). In contrast, the LPA>20µm condition was associated with higher relative abundances of rhamnose, fucose, arabinose, and galactose. The PCA of PAA>20µm further indicated that GABA, tyrosine, phenylalanine, and glutamic acid were the main contributors under LPA>20µm conditions, whereas the enrichment of arginine and aspartic acid characterized most samples associated with HPA>20µm conditions.

3.4 Species-specific correlations

To investigate potential links between phytoplankton species and major biomolecules, we conducted a correlation analysis between species-associated biomass and the biomolecular composition of carbohydrates and amino acids within the particulate (>20µm) and total fraction and for surface/SML as well as ULW-Net/ULW.

Dinophysis acuminata, *Dinophysis* (group) and *Chaetoceros sp.* were excluded from the correlation matrix due to their low and abundance.

https://doi.org/10.5194/egusphere-2025-5385
Preprint. Discussion started: 18 November 2025

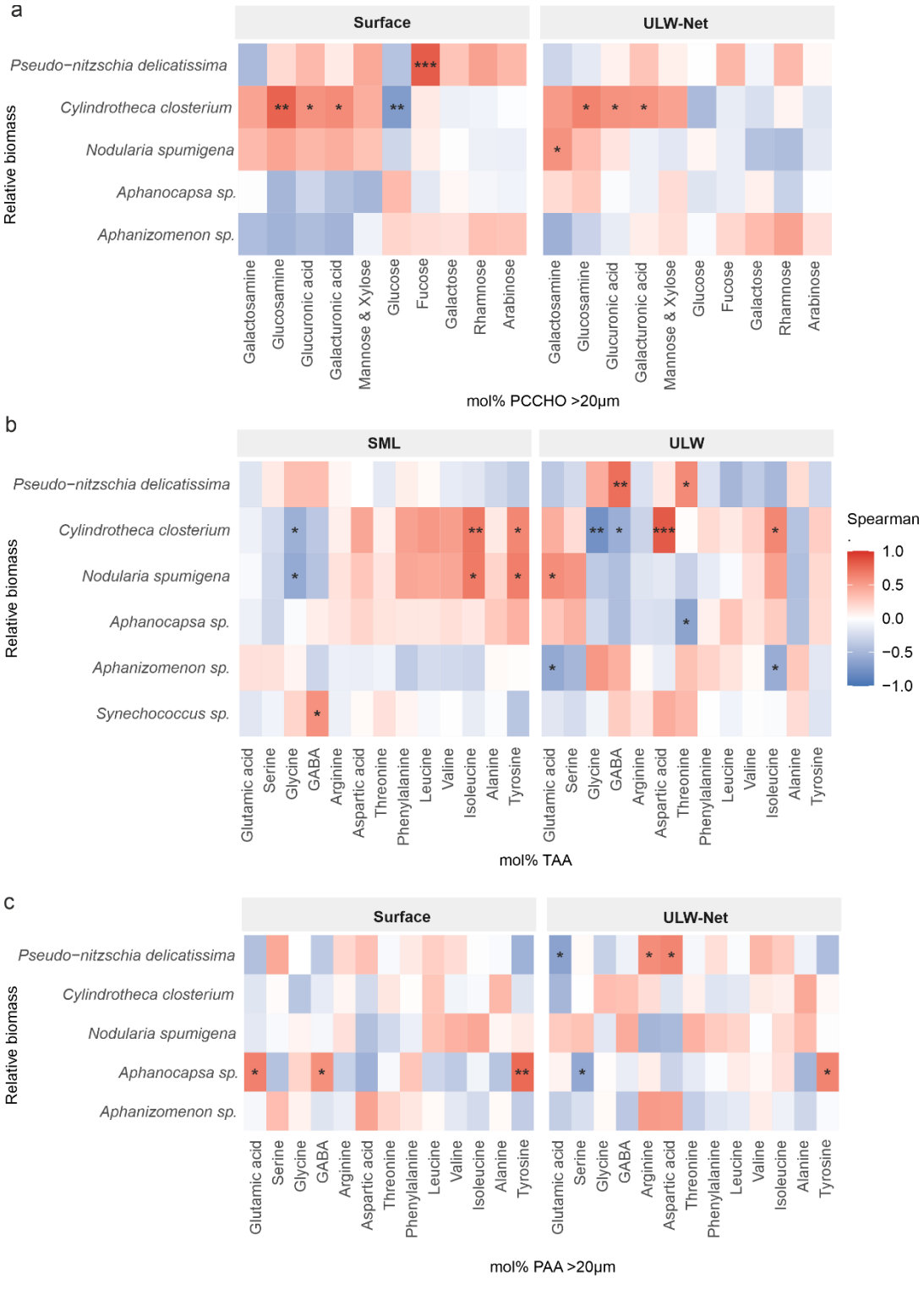

https://doi.org/10.5194/egusphere-2025-5385
Preprint. Discussion started: 18 November 2025

Figure 9: Heatmaps of Spearman rank-order correlations (ρ) between relative phytoplankton biomass and mol% of (a) particulate combined carbohydrates (PCCHO>20µm), (b) total amino acids (TAA), and (c) particulate amino acids (PAA>20µm) in the surface/SML (left) and ULW-Net/ULW (right). Carbohydrates and amino acids have been reordered by hierarchical clustering to group positively- and negatively-associated carbohydrates and amino acids. Tile colors range from blue (ρ = –1) through white (ρ = 0) to red (ρ = +1), and significant correlations are marked with asterisks (* p < 0.05; ** p < 0.01; *** p < 0.001). Correlations with biomass of *Synchococcus sp.* were only performed for TAA.

For TCCHO, no positive correlations with phytoplankton species were found (Fig. S9). The relative biomass of the diatom *Cylindrotheca closterium* (biomass) correlated significantly negatively with total glucosamine (ρ = -0.60, p = 0.03), fucose (ρ = -0.60, p = 0.03) and rhamnose (ρ = -0.55, p = 0.05) in the SML and in the ULW with total fucose (ρ = -0.66, p = 0.01).

For PCCHO>20µm, significant correlations with individual phytoplankton species were observed (Fig. 9b). In the surface, the biomass of *Cylindrotheca closterium* showed the strongest positive correlation with particulate glucosamine (ρ = 0.79, p = 0.0013), followed by positive correlations with particulate glucuronic (ρ = 0.57, p = 0.044) and galacturonic (ρ = 0.60, p = 0.031) acid (Fig. 9a). Furthermore, in the surface, *Pseudo-nitzschia delicatissima* biomass was significantly correlated with particulate fucose (ρ =0.82, p = 0.0006). *Cylindrotheca closterium* biomass was negatively correlated with particulate glucose (ρ = -0.71, p = 0.0067). Other phytoplankton groups exhibited weaker or non-significant correlations in the surface. In the ULW-Net, *Cylindrotheca closterium* retains its positive, although weaker, correlation to particulate glucosamine (ρ = 0.64, p = 0.018), glucuronic acid (ρ =0.57, p = 0.044), and galacturonic acid (ρ =0.55, p = 0.049).

Among TAA (Fig. 9b), *Nodularia spumigena* and *Cylindrotheca closterium* revealed similar correlation. For both, positive correlations were observed in the SML with total isoleucine (ρ =0.68, p = 0.01; ρ =0.62, p = 0.024), and tyrosine (ρ =0.66, p = 0.013; ρ =0.62, p = 0.024) and a negative correlation with total glycine. *Aphanizomenon sp*. correlated negatively with total glutamic acid (ρ = -0.60, p = 0.029) and total isoleucine (ρ = -0.58, p = 0.039). *Synechococcus sp.* biomass showed the only positive correlation in the SML with GABA (ρ =0.57, p = 0.041). In the ULW, *Nodularia spumigena* biomass showed positive association with total glutamic acid (ρ =0.59, p = 0.035), different from the SML. *Cylindrotheca closterium* biomass correlated highly positively with total aspartic acid (ρ =0.84, p = 0.00038) and less strongly with isoleucine (ρ =0.69, p = 0.0087), but negatively with total glycine (ρ = -0.78, p = 0.0017) and GABA (ρ = -0.57, p = 0.044). *Pseudo-nitzschia delicatissima* biomass showed positive correlation with total GABA (ρ = 0.74, p = 0.0038) and total threonine (ρ = 0.61, p = 0.028), while a negative correlation with total threonine (ρ = -0.65, p = 0.017) was observed for *Aphanocapsa sp*. biomass.

Further, *Aphanocapsa sp*. showed the only statistically significant positive associations in the surface with PAA>20µm (Fig. 9c). Its biomass correlated positively with particulate glutamic acid (ρ = 0.65, p = 0.017), GABA (ρ = 0.58, p = 0.039) and strongest with tyrosine (ρ = 0.76, p = 0.0024) (Fig. 9c). No other phytoplankton taxa exhibited significant correlations with any PAA>20µm in the surface. In the ULW-Net, two taxa displayed weak but significant positive links. *Pseudo-nitzschia delicatissima* biomass correlated with arginine (ρ = 0.58, p = 0.036) and aspartic acid (ρ = 0.63, p = 0.021), while *Aphanocapsa sp*. biomass correlated positively with tyrosine (ρ = 0.64, p = 0.019). Negative correlations appeared between *Pseudo-nitzschia delicatissima* biomass and total glutamic acid (ρ = -0.65, p = 0.016) and *Aphanocapsa* sp. biomass and total serine (ρ = -0.62, p = 0.025).

https://doi.org/10.5194/egusphere-2025-5385
Preprint. Discussion started: 18 November 2025

4. Discussion

4.1 Phytoplankton composition in the Central Baltic Sea

The overarching goal of this study was to determine whether phytoplankton dynamics are reflected in SML composition, with a specific focus on cyanobacteria. To contextualize biomolecular dynamics, changes in the dominant phytoplankton members throughout the cruise will be discussed first. About 96% of the biomass >20µm was contributed by cyanobacteria, with an estimated mean cyanobacteria biomass >20µm of 6.78 ± 8.45 µg C L^{-1}. *Aphanizomenon* sp., *Nodularia spumigena*, and *Aphanocapsa* sp. represented the dominant genera, with the first two typically occurring in filamentous life stages (Wasmund, 1997) and the latter forming non-filamentous colonies (Komárek, 2003). *Nodularia* and *Aphanizomenon* were also shown to generally represent the dominant genera during the Baltic Sea summer in the Eastern Gotland Basin (Ploug, 2008; Zettler et al., 2024; HELCOM, 2025). During our cruise, *Aphanizomenon sp*. showed a mean biomass of 3.17 ± 3.43 µg C L^{-1} and *Nodularia spumigena* of 3.31 ± 5.25 µg C L^{-1}. This is lower than the estimate by Karlson et al. (2022), who reported a mean summer biomass of 15 µg C L^{-1} for both genera from the period 2000 – 2020. Wasmund (1997) suggested that, based on data collected from 1979–1993 in the Baltic proper and addressing *Aphanizomenon sp*. as the dominant genus, a biomass of up to 22 µg C L^{-1} (200 µg L^{-1} wet weight) can still be considered as a background concentration, while everything above should be defined as a bloom. According to the HELCOM report (2025), the recent mean of cyanobacteria biomass from June to August (2000 – 2023) was slightly below the long-term mean of 220 µg L^{-1} (wet weight), which corresponds to the bloom threshold set by Wasmund (1997) for *Aphanizomenon sp*.. Overall, in comparison to previous published values, our species-specific biomass estimates for *Aphanizomenon* and *Nodularia* are in the same order of magnitude and, following the interpretation of Wasmund (1997), do not align with bloom conditions. Cyanobacteria biomass sampled here made up 5.4 to 28.5% (mean: 12.7 %) of the POC>20µm, which was on average 4.4 ± 5.3 µM. Nausch et al. (2002) reported a mean surface POC concentration of 26.8 µM for the Baltic Sea, however, including all particles >0.7 µm. Likely, our cruise was slightly too early in the year to catch the summer blooms and we witnessed only the beginning accumulation of cyanobacteria biomass. In general, the spatial pattern of cyanobacteria accumulations on the surface is extremely patchy, as documented from remote-sensing and field studies (Kahru et al., 1994; Kutser, 2004; Seppälä et al., 2007; Karlson et al., 2022). A recent paper from Kahru et al. (2025) showed the frequency of the occurrence of cyanobacteria blooms from June to August during 2000–2024. For the area where our cruise was conducted, they found that roughly every fifth year no major accumulation of cyanobacterial biomass occurred. Additionally, they suggested that instead of sea surface temperature, surface irradiance causes the initiation of such blooms, implying that temporal seasonal offsets in the accumulation of biomass might occur in dependence on weather dynamics.

The Chl *a* concentration detected in this study (2.06 ± 0.35 µg L^{-1}) was lower than later in the same year (3.23 µg L^{-1}, August 2022), and close to our research area during a subsequent EMB298 cruise (Zettler et al., 2024). However, Bunse et al. (2019) noted Chl *a* concentrations similar to ours, and ranging from 1.68 to 2.41 µg L^{-1} during the summer months (June-September) in 2011 to 2014 west of Gotland. Our data showed that Chl *a* concentration increased over time from 1.63 ± 0.015 µg L^{-1} to

https://doi.org/10.5194/egusphere-2025-5385
Preprint. Discussion started: 18 November 2025

2.47 ± 0.1 µg L^{-1}. In parallel, also smaller phytoplankton <20µm cells increased during our cruise. Other studies reported that picophytoplankton can significantly contribute to Chl *a* (Sondergaard, 1991; Stal et al., 1999; Ohlendieck et al., 2000; Stal, 2003; Tamm et al., 2018). We found an overall phytoplankton <20µm cell abundance of 686 ± 458 x 10^3 cells mL^{-1} based on flow cytometry for the Central Baltic Sea. This is comparable to other studies, which found picocyanobacteria abundances of 150 to 550 x 10^3 cells mL^{-1} during summer (Albertano et al., 1997; Mazur-Marzec et al., 2013). In June 2015, a study in the Gotland Basin observed phytoplankton (including phycoerythrin- and Chl *a*-rich pico- and nanoplankton) abundances of ~ 96 x 10^3 cells mL^{-1} at 1m depth (Cisternas-Novoa et al., 2019), which are in line with our cell counts of the ULW (68 ± 41 x 10^3 cells mL^{-1}). Zufia et al. (2021) established that the abundance of phycoerythrin-rich picophytoplankton peaked during summer, which was consistent with other Baltic Sea studies (Mazur-Marzec et al., 2013; Larsson et al., 2014; Tamm et al., 2018). Overall, phytoplankton <20 µm abundances fell within the expected range for Baltic Sea summer conditions.

To compare the biomass of *Synechococcus sp.* with other studies, we estimated their biomass based on cell counts. Reported estimates of *Synechococcus* cellular carbon content range from 0.1 to 1.5 pg C $cell^{-1}$ (Moisan et al., 2010). Here, we used an average carbon content of 0.3 pg C $cell^{-1}$ based on Buitenhuis et al. (2012) and also applied by Hepach et al. (2020) for the Baltic Sea. We calculated an overall average *Synechococcus* biomass of 12.63 ± 12.18 µg C L^{-1}, which did not differ between SML and ULW. The elevated *Synechococcus sp.* biomass during HPA<20µm is comparable to other biomass values found for picoplankton during summer (Paczkowska et al., 2017). Additionally, Paczkowska et al. (2017) investigated that during summer (August), picocyanobacteria were the dominant size group, forming 40-90% of the total biomass in all basins of the Baltic Sea. This aligns with our findings, which show that, especially during HPA<20µm, *Synechococcus sp.* biomass was significantly higher than that of filamentous cyanobacteria-dominated HPA>20µm. Other studies also align with these findings (Andersson et al., 1996; Hajdu et al., 2007), and report a *Synechococcus* contribution of 65% to phytoplankton biomass in the Baltic Proper with nitrogen-fixing cyanobacteria (*Aphanizomenon spp.* and *Nodularia spp.*) being the second dominant group (Stal et al., 1999).

4.2 General SML dynamics in dependence of phytoplankton composition

Although the associated phytoplankton >20µm biomass reported here does not indicate the presence of a typical cyanobacteria bloom, phytoplankton members and biomass dynamically changed throughout the cruise. Dominant phytoplankton members were represented by filamentous, colonial and unicellular cyanobacteria. The phytoplankton community potentially influenced the organic matter pool as clear differences in biomolecular concentrations were revealed between depths (SML vs. ULW) and conditions (HPA>20µm vs. LPA>20µm). The highest average EF was detected for TAA (1.2 ± 0.4), while TCCHO and TOC exhibited EFs of approximately 1, independent of phytoplankton abundance. Previously reported EFs in the summerly western Baltic Sea averaged around 1.1 for dissolved and particulate amino acids (Barthelmeß and Engel, 2022). At the western Baltic Sea time series station Boknis Eck, an earlier study reported great seasonal variability of TAA and TCCHO concentrations and SML enrichment during two consecutive years, however, with EFs ranging between 0.8 and 1.2 (Dreshchinskii and Engel, 2017). TAA concentrations in the SML peaked in autumn with a maximum EF of 2.4 (Dreshchinskii and Engel, 2017), which

https://doi.org/10.5194/egusphere-2025-5385
Preprint. Discussion started: 18 November 2025

is comparable to the highest EF reported in this study. A recent meta-analysis revealed that pronounced enrichment of organic matter in the SML is rather uncommon, while nitrogen-containing biomolecules, including amino acids, preferentially accumulate in the SML (Silva et al., 2025, under review). The enrichments of TAA and TCCHO in the SML of the Central Baltic Sea found in this study are thus in line with previous reports and further emphasize that SML enrichment patterns are compound-specific. At the time series station Boknis Eck, only one SML sample showed TAA concentration >3.0 µM during two consecutive years (Dreshchinskii and Engel, 2017). Hence, TAA concentrations in the Central Baltic Sea, (e.g. with a mean of 3.85 ± 1.52 µM in the SML during HPA>20µm) were thus substantially higher than previously observed in the Western Baltic Sea.

The enrichment of surfactants in the SML differed in dependence of phytoplankton abundance, as the EF during HPA<20µm (1.1 ± 0.2; median = 1.1) exceeded the EF during LPA<20µm (1.1 ± 0.2; median = 1.0). During HPA<20µm, we further measured the highest surfactant concentrations (0.56 ± 0.09 mg L^{-1} TX-100 equiv.) in the SML. In line with our results, averaged EFs of surfactants ranged between 0.9 and 1.4 in coastal regimes of the North Sea and Baltic Sea (Stolle et al., 2020; Barthelmeß and Engel, 2022). EFs of surfactants are generally lower in eutrophic regimes (Wurl et al., 2011), such as the Baltic Sea. However, exceptionally high surfactant concentrations may occur in coastal regions or under specific oceanic conditions at low wind regimes and tend to condense into visible surface slicks, exceeding a concentration of 0.65 mg/ L equiv. TX-100 (Wurl et al., 2016; Sabbaghzadeh et al., 2017; Mustaffa et al., 2020). Depending on the region and season, previously reported surfactant concentrations in coastal seas differ considerably. For the SML in a coastal transect off North East England, the authors reported a seasonal minimum and maximum of 0.08 and 0.38 mg/ L equiv. TX-100, respectively (Pereira et al., 2016). During spring, diel variability of SML surfactant concentrations ranged between 0.17 and 0.26 mg/ L equiv. TX-100 at a coastal station of the North Sea (Stolle et al., 2020). In the Western Baltic Sea, SML surfactant concentrations varied between 0.28 and 0.49 mg/ L equiv. TX-100 during two consecutive seasons (Barthelmeß and Engel, 2022). Estuarian and riverine surfactant concentrations, in contrast, frequently exceeded 1.00 mg/ L equiv. TX-100 (Rickard et al., 2022). In summary, surfactant concentrations reported here were rather high in comparison to coastal stations (Barthelmeß and Engel, 2022).

Although, TOC enrichment was close to 1, concentrations varied significantly with depth during HPA<20µm (Fig. S6d). The average TOC concentrations in the SML presented here was 398 ± 23 µM. TOC and DOC concentrations in the Baltic Sea are comparable, as POC constitutes only a minor fraction of TOC (Stråat et al., 2016). In the Baltic Proper, it is estimated that 74 to 77% of DOC in spring and autumn, respectively, can be attributed to riverine input (Seidel et al., 2017). DOC concentrations steadily decline towards the Western Baltic Sea due to mixing with inflowing North Sea water, also reducing the contribution of terrestrial DOC (Seidel et al., 2017). Within the Western Gotland Sea, DOC concentration exhibited a seasonal range of 327 to 472 µM (mean 361 µM), while peaking during the summer months, reflected by an increase of ~50 µM (Bunse et al., 2019). This summer increase is potentially associated with autochthonous production (Seidel et al., 2017). Depending on the season and region, TOC concentrations in the Baltic Sea are exceptionally high in comparison to other coastal seas, and due to the high terrestrial DOC. In summary, the general SML enrichment pattern as well as carbohydrate concentrations aligned with previous results reported from the Western Baltic Sea or elsewhere. TAA and surfactant concentrations, however, were

https://doi.org/10.5194/egusphere-2025-5385
Preprint. Discussion started: 18 November 2025

notably elevated in the Central Baltic Sea in comparison to the Western Baltic Sea. Summerly TOC variability can likely be attributed to phytoplankton production.

4.3 Specific biomolecular pattern associated with distinct phytoplankton members

In line with categorizing phytoplankton into high and low abundance (and corresponding to high and low cyanobacteria biomass), POC, PAA and PCCHO >20µm concentration were highest in the ULW-Net during HPA>20µm. PAA and PCCHO >20µm contributed on average 12.9 ± 6.4% and 10.1 ± 2.3% to POC>20µm, respectively. This corresponds roughly to the proportion of amino acids and carbohydrates reported for particulate organic matter in the surface ocean (~30%, pore size ~0.4µm, Kaiser and Benner, 2009). Cell-based phytoplankton biomass estimates and measured POC>20µm concentrations diverged considerably, as the biomass contributed only 13.5 ± 6.1 % to POC>20µm concentrations. Satellite and in-situ observations corroborate that phytoplankton biomass in temperate and more productive regimes substitutes between 10 to 30% of POC only (Arteaga et al., 2016). The residual POC, which was not explained by the apparent biomass, can be attributed to heterotrophic plankton, and detritus, including extracellular material constituting the filamentous and colonial lifestyle of cyanobacteria, and gel-like particles (Mari and Kiørboe, 1996; Engel et al., 2004; Pannard et al., 2016, Cisternas-Novoa et al. 2019). The observed correlation between POC>20µm and cellular biomass >20µm indicates that particulate organic matter was largely associated with cyanobacteria, including detrital and extracellular components. During this study, POC>20µm concentration was related to cyanobacterial cellular biomass >20µm (HPA>20µm: 1.6 ± 1.7; LPA>20µm: 0.7 ± 0.7%), confirming the assumption that filamentous or colonial cyanobacteria influence the particulate organic matter pool of the Central Baltic Sea and in spite the absence of a bloom. PAA accounted for a significantly larger proportion of TAA under HPA>20µm (5.4 ± 4.8%) than under LPA>20µm conditions (1.9 ± 1.9%). In contrast, the overall contribution of PCCHO to TCCHO (1.3 ± 1.2%) and the difference between conditions were considerably smaller.

PAA showed high fractions of the amino acid arginine in comparison to TAA (Fig. 7d). Arginine defined a specific cluster of the HPA>20µm community (PCA Fig. 8d), and was associated with *Pseudo-nitzschia delicatissima*. The fraction of arginine in the PAA pool (>20µm) of the Central Baltic Sea was particularly higher than in the Western Baltic Sea (Barthelmeß & Engel, 2022). Moreover, PCCHO>20µm was composed of elevated fractions of glucose and glucuronic acid in comparison to the total fraction (Fig. 7a, b). While particulate glucose defined cyanobacteria (>20µm) during HPA>20µm and LPA>20µm conditions equally (Fig. 8b), elevated ratios of glucuronic acid, glucosamine, galacturonic acid, and galactosamine aligned with HPA>20µm conditions (Fig. 8b) and further correlated with *Cylindrotheca closterium* and *Nodularia spumigena* (Fig. 9a), of which the later constituted the higher biomass. The higher percentage of particulate glucose is characteristic for productive regimes (Engel et al., 2012; Barthelmeß and Engel, 2022). HPA<20µmdominated by *Synechococcus sp.* , on the other hand, aligned with galactose (Fig. 8a, c) and elevated ratios of the non-proteinogenic amino acid GABA (Fig. 9b), which is often associated with advanced heterotrophic degradation (Dauwe et al., 1999; Davis et al., 2009; Barthelmeß and Engel, 2022).

https://doi.org/10.5194/egusphere-2025-5385
Preprint. Discussion started: 18 November 2025

As outlined above, the contributions of large (>20µm) and small (<20µm) phytoplankton members were notably reciprocal. The co-occurrence of specific phytoplankton taxa is not random but potentially relates to trophic or allelopathic interactions, such as the transfer of newly fixed nitrogen from filamentous cyanobacteria to diatoms (Chen et al., 2011) or species-specific selection via the release of allelochemicals. *Nodularia spumigena* may cause a decline in growth and physical cell damage to specific diatoms by the release of toxins (Śliwińska-Wilczewska et al., 2019), or be adversely affected by diatoms (Lage et al., 2022). In the later study, co-culturing resulted in an upregulated release of specific peptides by *Nodularia. spumigena*. Allelopathic interaction between Baltic strains of cyanobacteria has been also observed, such as a multifactorial growth suppression of *Nodularia spumigena* by *Synechococcus sp.* (Barreiro Felpeto et al., 2018). Allelopathic effects may thus explain why reciprocal patterns were found for the categorization of phytoplankton abundance into larger and smaller cells (20µm) i.e. elevated contributions of *Synecococcus sp*. cooccurred with decreased cyanobacterial biomass in 10 out of 13 sample sets. To summarize, specific biomolecular patterns of the SML could be associated with the particulate fraction and the occurrence of filamentous and colonial cyanobacteria, as well as with the total fraction and the predominant occurrence of picophytoplankton (*Synechococcus sp*.), respectively.

4.4 The influence of cyanobacteria on the ambient organic matter pool

The reciprocal pattern of the occurrence of small and large cyanobacteria further allows to determine whether filamentous and colonial or unicellular cyanobacteria potentially exhibit a biomolecular imprint on the organic matter. In figure 8a, galactose and glucose defined the main variance along PC1 (TCCHO). While the former represented HPA<20µm conditions, the latter aligned with HPA>20µm conditions. The variance along PC2 was associated with glucuronic acid and further influenced samples related to HPA>20µm conditions. As previously noted, glucose and glucuronic acid defined major differences between the PCCHO (>20µm) and TCCHO pool. The described pattern can therewith be interpreted as a subtle biomolecular imprint of large cyanobacteria on the ambient TCCHO pool. In Figure 9b, the main variance along PC1 was defined by a bundle of amino acids (incl. arginine, leucine, phenylalanine), which are often associated with fresher material from the surface ocean and opposed by glutamic acid, serine and glycine of which the latter two define degraded rather than freshly produced organic matter (Dauwe et al., 1999; Kaiser and Benner, 2009). Amino acids characteristic of fresher material were thus associated with the ULW (Fig. S8). Data separated only into the defined categories of HPA and LPA<20µm along PC2, which explained considerably less variance of the TAA data. While *Synechococcus sp*. occurred in similar abundances in both the SML and ULW, filamentous and colonial cyanobacteria dominated in the ULW during HPA>20µm. Tentatively, a biomolecular imprint of large cyanobacteria defined by predominantly arginine and leucine (PAA, Fig. 8d) can thus be detected along PC2.

Heterocystous cyanobacteria, such as *Nodularia sp.* and *Aphanizomenon sp.* are a monophyletic group (Tomitani et al., 2006). Filamentous and colonial cyanobacteria with the ability to fixate atmospheric nitrogen accumulate cyanophycin within their heterocysts. Cyanophycin is a polymer composed of arginine and aspartate (Flores et al., 2019). Specific anabolic pathways using the four nitrogen atoms of arginine therewith establish cyanophycin as a liable nitrogen reservoir in heterocystous

https://doi.org/10.5194/egusphere-2025-5385
Preprint. Discussion started: 18 November 2025

cyanobacteria during unbalanced growth conditions (Flores et al., 2019) and may explain the particularly high fraction of arginine in the PAA>20µm pool as well as its subtle influence on the composition of the ULW (TAA). While cyanobacteria accumulate cyanophycin within their heterocysts (Flores et al., 2019), these specialized cells rely on the supply of carbohydrates from adjacent vegetative cells (Nürnberg et al., 2015; Stuart et al., 2016). Interestingly, glucose dominates this intercellular trophic exchange and further constitutes the associated extracellular material (Nürnberg et al., 2015; Stuart et al., 2016). Within cyanobacterial mats, glucose polymers are made available by the release of extracellular enzymes (Stuart et al., 2016). In accordance, an increased fraction of uronic acids and amino sugars has been attributed to aid EPS aggregation as summarized by Engel et al. (2020). Glucose, amino sugars and uronic acids were elevated in PCCHO>20µm and associated to HPA>20µm and thus characterized in particular the extracellular material of the filamentous and colonial cyanobacteria, which is further inhabited by a rich heterotrophic community. Heterotrophic bacteria profit from the extracellular and aggregated resources, likewise replenishing the pool of extracellular proteins further (Stuart et al., 2016). To conclude, we found that both phytoplankton size fractions influenced the ambient total organic matter pool, as evident from specific biomolecular contributions, which can likely be explained by trophic and allelopathic interactions.

4.5 How surfactants relate to biomolecular dynamics

In general, elevated surface activity has been associated with both the particulate and dissolved fraction as well as with fresh and degraded organic matter profiles (Zutic et al., 1981; Engel et al., 2018b; Barthelmeß and Engel, 2022). As summarized by Barthelmeß and Engel (2022), amino acids accumulating in the SML are usually characterized by a higher polarity and are represented by arginine, glutamic acid, and serine. This is again supported by the data presented here, as the amino acids serine and glutamic acid seemed to be relatively more abundant in the SML. Heterotrophic bacteria release surfactants to enhance substrate availability and uptake (Satpute et al., 2010) and explicitly arginine has been suggested as a potent candidate to enhance surface activity (Engel et al., 2018b). While relatively higher fractions of arginine accompanied the predominant occurrence of large cyanobacteria in the ULW-Net, surfactant concentrations were higher within the SML under the prevalence of the small cyanobacteria *Synechococcus sp.* (HPA<20µm). Higher surfactant enrichment has been shown to occur in alignment with advanced organic matter degradation (Wurl et al., 2011; Barthelmeß and Engel, 2022). GABA characterized the organic matter pool during HPA<20µm and has been associated with, first, advanced bacterial processing (Davis et al., 2009) and, second, the accumulation of surfactants at the air-sea interface (Engel et al., 2018b). Here, we found also elevated fractions of galactose and concentrations of *Synechococcus sp*. biomass (20.59 ± 15.17 µg C L^{-1}) as well as Chl *a* during HPA<20µm. This indicates that a system is typically dominated by phytoplankton production rather than bacterial degradation. *Synechococcus sp*. has been shown to form CSP-rich aggregates (Cisternas-Novoa et al., 2015). Given the proteinaceous nature of CSP, amino acids and other surface-active organic compounds likely act as precursors for their formation, with hydrophobic amino acid side chains facilitating aggregation at in the SML (Wurl & Holmes, 2008; Cunliffe et al., 2013; Thornton et al., 2016, 2018). In conclusion, we suggest that the surfactant pools during our study were dominated by elevated phytoplankton production in contrast to heterotrophic microbial processing, respectively. Moreover, it should be taken into consideration that

https://doi.org/10.5194/egusphere-2025-5385
Preprint. Discussion started: 18 November 2025

the Central Baltic Sea harbours a rich reservoir of microbially altered terrestrial material, while also abiotic factors such as solar radiation (Rickard et al., 2022) or anthropogenic pollutants may alter surface activity (Wurl and Obbard, 2004).

In comparison to the Western Baltic Sea, elevated amino acid concentrations in the Central Baltic Sea likely reflect the high biomass of filamentous and colonial cyanobacteria, whereas enhanced surfactant levels may be attributed to the small cyanobacteria *Synechococcus sp.* contributing to the surface-active organic matter pool. This is in line with Mustaffa et al. (2020), who encountered an extensive *Trichodesmium* sp. bloom in the open ocean Pacific, which provoked a slick-covered surface. Surfactant concentrations reported here were rather high in comparison to other coastal stations, suggesting a pronounced suppression of air-sea gas fluxes (Pereira et al., 2016; Mustaffa et al., 2020) and exceeding the effect size of the surfactant pool, which is present in the Western Baltic Sea (Barthelmeß and Engel, 2022).

5. Conclusion

This study examined whether phytoplankton dynamics are reflected in the composition of the sea surface microlayer (SML), focusing on filamentous cyanobacteria. Although no typical bloom occurred, the phytoplankton community varied dynamically throughout the cruise, resulting in clear differences in biomolecular composition between depths (SML vs. ULW) and high versus low cyanobacteria-dominated phytoplankton >20µm abundance (HPA>20µm vs. LPA>20µm). SML enrichment patterns and carbohydrate concentrations generally aligned with previous observations from the Western Baltic Sea, while total amino acid (TAA) and surfactant concentrations were notably higher in the Central Baltic Sea. This likely reflects enhanced phytoplankton production under a favourable salinity range (6–9 PSU), supporting filamentous cyanobacteria, and unlike the more saline Western Baltic Sea (>12 PSU). Distinct biomolecular signatures indicated contributions from both large and small phytoplankton. Elevated total combined carbohydrate (TCCHO) concentrations during HPA<20µm suggest that smaller phytoplankton, such as *Synechococcus sp.*, drove carbohydrate and surfactant production, whereas the tendency to higher TAA and PAA concentrations during HPA>20µm point to a stronger influence of cyanobacteria on proteinaceous material. Compared to the Western Baltic Sea, elevated surfactant and amino acid concentrations, along with the observed biomolecular imprints, indicate that cyanobacteria have a strong influence on the organic matter and surfactant pool in the Central Baltic Sea.

Appendix A

Table A 1: Overview of stations sampled during EMB295 cruise. A cross for each station was set when sampling of particulate matter >20µ with the Neuston catamaran (cat) and ULW net. It is indicated when SML sampling took place with glass plate or Garrett Screen and ULW sampling with the manually conducted Niskin bottle. Moring and afternoon sampling took place at each station, except for the first and last station.

Station	Date	Time [local time]	Catamaran	ULW net	Glas Plate	Garrett Screen	Manuel Niskin Bottle

https://doi.org/10.5194/egusphere-2025-5385
Preprint. Discussion started: 18 November 2025

12-03	06.07.2022	16:17:00	x	x		x	x
12-07	07.07.2022	04:00:00	x	x		x	x
12-11	07.07.2022	16:12:00	x	x		x	x
12-16	08.07.2022	04:26:00	x	x	x		x
12-24	08.07.2022	19:20:00	x	x		x	x
12-27	09.07.2022	04:29:00	x	x	x		x
13-03	09.07.2022	16:10:00	x	x	x		x
14-01	10.07.2022	04:16:00	x	x		x	x
14-05	10.07.2022	18:15:00	x	x	x		x
17-02	11.07.2022	04:20:00	x	x	x		x
18-02	11.07.2022	14:40:00	x	x		x	x
21-02	13.07.2022	13:58:00	x	x	x		x
22-02	15.07.2022	04:18:00				x	x
22-04	15.07.2022	16:19:00				x	x
22-07	16.07.2022	04:59:00	x	x	x		x

Table A 2: Classification of stations according to phytoplankton >20µm and <20µm abundance.

Station	Date	Biomass classification	Abundance classification
12-03	06.07.2022	HPA>20µm	LPA<20µm
12-07	07.07.2022	HPA>20µm	LPA<20µm
12-11	07.07.2022	LPA>20µm	LPA<20µm
12-16	08.07.2022	HPA>20µm	LPA<20µm
12-24	08.07.2022	HPA>20µm	LPA<20µm
12-27	09.07.2022	LPA>20µm	HPA<20µm
13-03	09.07.2022	HPA>20µm	LPA<20µm
14-01	10.07.2022	LPA>20µm	LPA<20µm
14-05	10.07.2022	HPA>20µm	LPA<20µm
17-02	11.07.2022	LPA>20µm	HPA<20µm
18-02	11.07.2022	LPA>20µm	HPA<20µm
21-02	13.07.2022	HPA>20µm	HPA<20µm
22-02	15.07.2022	na	HPA<20µm
22-04	15.07.2022	na	HPA<20µm
22-07	16.07.2022	LPA>20µm	HPA<20µm

https://doi.org/10.5194/egusphere-2025-5385
Preprint. Discussion started: 18 November 2025

Data availability

The data presented in this study will be submitted to the PANGAEA Data Publisher for Earth & Environmental Science and will be made publicly available after publication of the manuscript.

Author contributions

JK collected samples during the research cruise, performed surfactant analyses, conducted data analysis, and wrote and prepared the manuscript. AE designed the project, supervised the research, and contributed to manuscript writing and revision. TB assisted with data analysis, contributed to manuscript writing, and participated in manuscript revision. BS supported sample collection and filtration during the cruise and contributed to manuscript proofreading.

Competing interests

The authors declare that they have no conflict of interest.

Disclaimer

Special issue statement

Acknowledgments

We sincerely thank the chief scientist Henry Bittig and the senior scientist Christa Marandino for their exceptional efforts in organizing the research cruises and supporting the implementation of our extensive SML sampling program. We are grateful to Mathis Björner for his assistance with SML sampling on the working boat and, together with Michael Glockzin (IOW), for operating the CTD. We also extend our appreciation to the captain and crew of the RV *Elisabeth Mann Borgese* for their dedicated support throughout the cruise operations.

We further thank Tania Klüver, Jon Roa, and Ruth Flerus for analyzing a substantial portion of the samples in our home laboratory. Our gratitude goes to Christian Burmeister for chlorophyll *a* measurements, Lars Kreuzer for nutrient analyses, and Joanna Waniek and Prof. Heide Schulz-Vogt (IOW) for generously providing laboratory access. We also acknowledge AquaEcology GmbH & Co. KG for conducting the microphytoplankton analyses.

https://doi.org/10.5194/egusphere-2025-5385
Preprint. Discussion started: 18 November 2025

Financial support

This research was supported by the project "Biogeochemical processes and Air–sea exchange in the Sea–Surface microlayer (BASS)", which was funded by the German Research Foundation (DFG) under Grant No 451574234.

References

Abdelgadir, M., Broman, E., Dinnétz, P., Olofsson, M., and Sjöling, S.: Future increase of filamentous cyanobacteria in coastal Baltic Sea predicted by multiple realm models of marine, terrestrial, and climate change scenarios, Ecol Inform, 92, https://doi.org/10.1016/j.ecoinf.2025.103439, 2025.

Abraham, W. R., Meyer, H., and Yakimov, M.: Novel glycine containing glucolipids from the alkane using bacterium Alcanivorax borkumensis, Biochimica et Biophysica Acta (BBA) - Lipids and Lipid Metabolism, 1393, 57–62, https://doi.org/10.1016/S0005-2760(98)00058-7, 1998.

Albertano, P., Somma, D. Di, and Capucci, E.: Cyanobacterial picoplankton from the Central Baltic Sea: cell size classification by image-analyzed fluorescence microscopy, J Plankton Res, 19, 1405–1416, https://doi.org/10.1093/plankt/19.10.1405, 1997.

Andersson, A., Hajdu, S. and Haecky, P.: Succession and growth limitation of phytoplankton in the Gulf of Bothnia (Baltic Sea). Oceanographic Literature Review, 10(44), p.1137, 1997

Arteaga, L., Pahlow, M., and Oschlies, A.: Modeled Chl:C ratio and derived estimates of phytoplankton carbon biomass and its contribution to total particulate organic carbon in the global surface ocean, Global Biogeochem Cycles, 30, 1791–1810, https://doi.org/10.1002/2016GB005458, 2016.

Barreiro Felpeto, A., Śliwińska-Wilczewska, S., Złoch, I., and Vasconcelos, V.: Light-dependent cytolysis in the allelopathic interaction between picoplanktic and filamentous cyanobacteria, J Plankton Res, 40, 165–177, https://doi.org/10.1093/plankt/fby004, 2018.

Barthelmeß, T. and Engel, A.: How biogenic polymers control surfactant dynamics in the surface microlayer: insights from a coastal Baltic Sea study, Biogeosciences, 19, 4965–4992, https://doi.org/10.5194/bg-19-4965-2022, 2022.

Barthelmeß, T., Schütte, F., and Engel, A.: Variability of the Sea Surface Microlayer Across a Filament's Edge and Potential Influences on Gas Exchange, Front Mar Sci, 8, https://doi.org/10.3389/fmars.2021.718384, 2021.

Buitenhuis, E. T., Li, W. K. W., Vaulot, D., Lomas, M. W., Landry, M. R., Partensky, F., Karl, D. M., Ulloa, O., Campbell, L., Jacquet, S., Lantoine, F., Chavez, F., MacIas, D., Gosselin, M., and McManus, G. B.: Picophytoplankton biomass distribution in the global ocean, Earth Syst Sci Data, 4, 37–46, https://doi.org/10.5194/essd-4-37-2012, 2012.

Bunse, C., Israelsson, S., Baltar, F., Bertos-Fortis, M., Fridolfsson, E., Legrand, C., Lindehoff, E., Lindh, M. V., Martínez-García, S., and Pinhassi, J.: High frequency multi-year variability in baltic sea microbial plankton stocks and activities, Front Microbiol, 10, https://doi.org/10.3389/fmicb.2018.03296, 2019.

Chen, Y. L. L., Tuo, S., and Chen, H. Y.: Co-occurrence and transfer of fixed nitrogen from Trichodesmium spp. to diatoms in the low-latitude Kuroshio Current in the NW Pacific, Mar Ecol Prog Ser, 421, 25–38, 2011.

https://doi.org/10.5194/egusphere-2025-5385
Preprint. Discussion started: 18 November 2025

Cisternas-Novoa, C., Le Moigne, F. A. C., and Engel, A.: Composition and vertical flux of particulate organic matter to the oxygen minimum zone of the central Baltic Sea: Impact of a sporadic North Sea inflow, Biogeosciences, 16, 927–947, https://doi.org/10.5194/bg-16-927-2019, 2019.

Cosović, B. and Vojvodić, V.: The application of ac polarography to the determination of surface-active substances in seawater, https://doi.org/10.4319/lo.1982.27.2.0361, Limnology and Oceanography 27.2, 361-369,1982.

Cunliffe, M. and Murrell, J. C.: The sea-surface microlayer is a gelatinous biofilm, ISME J, 3, 1001–1003, https://doi.org/10.1038/ismej.2009.69, 2009.

Cunliffe, M., Engel, A., Frka, S., Gašparović, B. Ž., Guitart, C., Murrell, J. C., Salter, M., Stolle, C., Upstill-Goddard, R., and Wurl, O.: Sea surface microlayers: A unified physicochemical and biological perspective of the air–ocean interface, Prog Oceanogr, 109, 104–116, https://doi.org/10.1016/J.POCEAN.2012.08.004, 2013.

Cunliffe, M. and Wurl, O., Guide to best practices to study the ocean's surface, 2014.

Cyanobacteria biomass 2000-2023. HELCOM Baltic Sea Environment Fact Sheets. HELCOM, 2025

Dauwe, B., Middelburg, J. J., Herman, P. M. J., and Heip, C. H. R.: Linking diagenetic alteration of amino acids and bulk organic matter reactivity, Limnol Oceanogr, 44, 1809–1814, https://doi.org/10.4319/lo.1999.44.7.1809, 1999.

Davis, J., Kaiser, K., and Benner, R.: Amino acid and amino sugar yields and compositions as indicators of dissolved organic matter diagenesis, Org Geochem, 40, 343–352, https://doi.org/10.1016/J.ORGGEOCHEM.2008.12.003, 2009.

Dickson, A. G. ., Sabine, C. L. ., and Christian, J. Robert.: Guide to best practices for ocean CO_2 measurements, North Pacific Marine Science Organization, 2007.

DIN EN 15972: Wasserbeschaffenheit - Anleitung für die quantitative und quali-tative Untersuchung von marinem Phytoplankton. Beuth Verlag, 34 Seiten, 2011.

DIN EN 16695: Wasserbeschaffenheit - Anleitung zur Abschätzung des Phyto-plankton-Biovolumens. Beuth Verlag, 101 Seiten., 2015.

Dittmar, T., Cherrier, J., and Ludwichowski, K.-U.: 4 The Analysis of Amino Acids in Seawater, n.d.

Dreshchinskii, A. and Engel, A.: Seasonal variations of the sea surface microlayer at the Boknis Eck Times Series Station (Baltic Sea), J Plankton Res, 39, 943–961, https://doi.org/10.1093/plankt/fbx055, 2017.

Endres, S., Unger, J., Wannicke, N., Nausch, M., Voss, M., and Engel, A.: Response of Nodularia spumigena to CO2-Part 2: Exudation and extracellular enzyme activities, Biogeosciences, 10, 567–582, https://doi.org/10.5194/bg-10-567-2013, 2013.

Engel, A. and Galgani, L.: The organic sea-surface microlayer in the upwelling region off the coast of Peru and potential implications for air-sea exchange processes, Biogeosciences, 13, 989–1007, https://doi.org/10.5194/bg-13-989-2016, 2016.

Engel, A. and Händel, N.: A novel protocol for determining the concentration and composition of sugars in particulate and in high molecular weight dissolved organic matter (HMW-DOM) in seawater, Mar Chem, 127, 180–191, https://doi.org/10.1016/J.MARCHEM.2011.09.004, 2011.

https://doi.org/10.5194/egusphere-2025-5385
Preprint. Discussion started: 18 November 2025

Engel, A., Delille, B., Jacquet, S., Riebesell, U., Rochelle-Newall, E., Terbrüggen, A., and Zondervan, I.: Transparent exopolymer particles and dissolved organic carbon production by Emiliania huxleyi exposed to different CO2 concentrations: a mesocosm experiment, Aquatic Microbial Ecology, 34, 93–104, 2004.

Engel, A., Harlay, J., Piontek, J., and Chou, L.: Contribution of combined carbohydrates to dissolved and particulate organic carbon after the spring bloom in the northern Bay of Biscay (North-Eastern Atlantic Ocean), Cont Shelf Res, 45, 42–53, https://doi.org/10.1016/j.csr.2012.05.016, 2012.

Engel, A., Bange, H. W., Cunliffe, M., Burrows, S. M., Friedrichs, G., Galgani, L., Herrmann, H., Hertkorn, N., Johnson, M., Liss, P. S., Quinn, P. K., Schartau, M., Soloviev, A., Stolle, C., Upstill-Goddard, R. C., van Pinxteren, M., and Zäncker, B.: The ocean's vital skin: Toward an integrated understanding of the sea surface microlayer, Frontiers in Marine Science, 4, 165.https://doi.org/10.3389/fmars.2017.00165, 30 May 2017.

Engel, A., Sperling, M., Sun, C., Grosse, J., and Friedrichs, G.: Organic matter in the surface microlayer: Insights from a wind wave channel experiment, Front Mar Sci, 5, https://doi.org/10.3389/fmars.2018.00182, 2018a.

Engel, A., Sperling, M., Sun, C., Grosse, J., and Friedrichs, G.: Organic matter in the surface microlayer: Insights from a wind wave channel experiment, Front Mar Sci, 5, https://doi.org/10.3389/fmars.2018.00182, 2018b.

Engel, A., Endres, S., Galgani, L., and Schartau, M.: Marvelous Marine Microgels: On the Distribution and Impact of Gel-Like Particles in the Oceanic Water-Column, Front Mar Sci, 7, https://doi.org/10.3389/fmars.2020.00405, 2020.

Flores, E., Arévalo, S., and Burnat, M.: Cyanophycin and arginine metabolism in cyanobacteria, Algal Res, 42, 101577, https://doi.org/10.1016/J.ALGAL.2019.101577, 2019.

Frew, N. M., Bock, E. J., Schimpf, U., Hara, T., Haußecker, H., Edson, J. B., McGillis, W. R., Nelson, R. K., McKenna, S. P., Uz, B. M., and Jähne, B.: Air-sea gas transfer: Its depedence on wind stress, small-scale roughness, and surface films, J Geophys Res Oceans, 109, https://doi.org/10.1029/2003JC002131, 2004.

Galgani, L. and Engel, A.: Accumulation of Gel Particles in the Sea-Surface Microlayer during an Experimental Study with the Diatom Thalassiosira weissflogii, International Journal of Geosciences, 04, 129–145, https://doi.org/10.4236/ijg.2013.41013, 2013.

Galgani, L. and Engel, A.: Changes in optical characteristics of surface microlayers hint to photochemically and microbially mediated DOM turnover in the upwelling region off the coast of Peru, Biogeosciences, 13, 2453–2473, https://doi.org/10.5194/bg-13-2453-2016, 2016.

Garrett, W. D.: Collection of slick-forming materials from the sea surface microlayer, https://doi.org/10.4319/lo.1965.10.4.0602, Limnology and Oceanography 10.4, 602-605, 1965.

Gašparović, B. and Ćosović, B.: Surface-active properties of organic matter in the North Adriatic Sea, Estuar Coast Shelf Sci, 58, 555–566, https://doi.org/10.1016/S0272-7714(03)00133-1, 2003.

Hajdu, S., Höglander, H., and Larsson, U.: Phytoplankton vertical distributions and composition in Baltic Sea cyanobacterial blooms, Harmful Algae, 6, 189–205, https://doi.org/10.1016/j.hal.2006.07.006, 2007.

https://doi.org/10.5194/egusphere-2025-5385
Preprint. Discussion started: 18 November 2025

Harvey, G. W. and Burzell, L. A.: A simple microlayer method for small samples, https://doi.org/10.4319/lo.1972.17.1.0156, Limnology and Oceanography 17.1, 156-157. 1972.

Hepach, H., Hughes, C., Hogg, K., Collings, S., and Chance, R.: Senescence as the main driver of iodide release from a diverse range of marine phytoplankton, Biogeosciences, 17, 2453–2471, https://doi.org/10.5194/bg-17-2453-2020, 2020.

Jenkinson, I. R., Seuront, L., DIng, H., and Elias, F.: Biological modification of mechanical properties of the sea surface microlayer, influencing waves, ripples, foam and air-sea fluxes, Elem Sci Anth 6, 26, https://doi.org/10.1525/elementa.283, 2018.

Kahru, M. and Elmgren, R.: Multidecadal time series of satellite-detected accumulations of cyanobacteria in the Baltic Sea, Biogeosciences, 11, 3619–3633, https://doi.org/10.5194/bg-11-3619-2014, 2014.

Kahru, M., Horstmann, U., and Rud, O.: Report Satellite Detection of Increased Cyanobacteria Blooms i n the Baltic Sea: Natural Fluctuation or Ecosystem Change?, Ambio, Royal Swedish Academy of Sciences, 1994.

Kahru, M., Cahill, B., Elmgren, R., and Rehder, G.: What initiates cyanobacterial blooms in the Baltic Sea?, Harmful Algae, 148, https://doi.org/10.1016/j.hal.2025.102924, 2025.

Kaiser, K. and Benner, R.: Biochemical composition and size distribution of organic matter at the Pacific and Atlantic time-series stations, Mar Chem, 113, 63–77, https://doi.org/10.1016/J.MARCHEM.2008.12.004, 2009.

Karlson, A. M. L., Duberg, J., Motwani, N. H., Hogfors, H., Klawonn, I., Ploug, H., Barthel Svedén, J., Garbaras, A., Sundelin, B., Hajdu, S., Larsson, U., Elmgren, R., and Gorokhova, E.: Nitrogen fixation by cyanobacteria stimulates production in Baltic food webs, Ambio, 44, 413–426, https://doi.org/10.1007/s13280-015-0660-x, 2015.

Karlson, B., Arneborg, L., Johansson, J., Linders, J., Liu, Y., and Olofsson, M.: A suggested climate service for cyanobacteria blooms in the Baltic Sea – Comparing three monitoring methods, Harmful Algae, 118, https://doi.org/10.1016/j.hal.2022.102291, 2022.

Komárek, J.: Coccoid and Colonial Cyanobacteria, Freshwater Algae of North America: Ecology and Classification, 59–116, https://doi.org/10.1016/B978-012741550-5/50004-0, 2003.

Kujawinski, E. B., Farrington, J. W., and Moffett, J. W.: Evidence for grazing-mediated production of dissolved surface-active material by marine protists, Marine chemistry 77.2-3, 133-142, 2002.

Kurata, N., Vella, K., Hamilton, B., Shivji, M., Soloviev, A., Matt, S., Tartar, A., and Perrie, W.: Surfactant-associated bacteria in the near-surface layer of the ocean, Sci Rep, 6, https://doi.org/10.1038/srep19123, 2016.

Kutser, T.: Quantitative detection of chlorophyll in cyanobacterial blooms by satellite remote sensing, Limnol Oceanogr, 49, 2179–2189, https://doi.org/10.4319/lo.2004.49.6.2179, 2004.

Lage, S., Mazur-Marzec, H., and Gorokhova, E.: Interspecific Interactions Drive Nonribosomal Peptide Production in Nodularia spumigena, Appl Environ Microbiol, 88, https://doi.org/10.1128/aem.00966-22, 2022.

Larsson, J., Celepli, N., Ininbergs, K., Dupont, C. L., Yooseph, S., Bergman, B., and Ekman, M.: Picocyanobacteria containing a novel pigment gene cluster dominate the brackish water Baltic Sea, ISME J, 8, 1892–1903, https://doi.org/10.1038/ismej.2014.35, 2014.

https://doi.org/10.5194/egusphere-2025-5385
Preprint. Discussion started: 18 November 2025

Laß, K., Bange, H. W., and Friedrichs, G.: Seasonal signatures in SFG vibrational spectra of the sea surface nanolayer at Boknis Eck Time Series Station (SW Baltic Sea), Biogeosciences, 10, 5325–5334, https://doi.org/10.5194/bg-10-5325-2013, 2013.

Lennartz, S. T., Lehmann, A., Herrford, J., Malien, F., Hansen, H. P., Biester, H., and Bange, H. W.: Long-term trends at the Boknis Eck time series station (Baltic Sea), 1957-2013: Does climate change counteract the decline in eutrophication?, Biogeosciences, 11, 6323–6339, https://doi.org/10.5194/bg-11-6323-2014, 2014.

Lindroth, P. and Mopper, K.: High Performance Liquid Chromatographic Determination of Subpicomole Amounts of Amino Acids by Precolumn Fluorescence Derivatization with o-Phthaldialdehyde, Analytical chemistry chemistry, UTC, 57 pp., 2025.

Marie, D., Partensky, F., Jacquet, S., and Vaulot, D.: Enumeration and Cell Cycle Analysis of Natural Populations of Marine Picoplankton by Flow Cytometry Using the Nucleic Acid Stain SYBR Green I, Appl Environ Microbiol, 63, 186–193, https://doi.org/10.1128/aem.63.1.186-193.1997, 1997.

Marie, D., Shi, X. L., Rigaut-Jalabert, F., and Vaulot, D.: Use of flow cytometric sorting to better assess the diversity of small photosynthetic eukaryotes in the English Channel, FEMS Microbiol Ecol, 72, 165–178, https://doi.org/10.1111/j.1574-6941.2010.00842.x, 2010.

Mari, X. and Kiørboe, T.: Abundance, size distribution and bacterial colonization of transparent exopolymeric particles (TEP) during spring in the Kattegat, J Plankton Res, 18, 969–986, https://doi.org/10.1093/plankt/18.6.969, 1996.

Mazur-Marzec, H., Sutryk, K., Kobos, J., Hebel, A., Hohlfeld, N., Błaszczyk, A., Toruńska, A., Kaczkowska, M. J., Łysiak-Pastuszak, E., Kraśniewski, W., and Jasser, I.: Occurrence of cyanobacteria and cyanotoxin in the Southern Baltic Proper. Filamentous cyanobacteria versus single-celled picocyanobacteria, Hydrobiologia, 701, 235–252, https://doi.org/10.1007/s10750-012-1278-7, 2013.

Moisan, T. A., Blattner, K. L., and Makinen, C. P.: Influences of temperature and nutrients on Synechococcus abundance and biomass in the southern Mid-Atlantic Bight, Cont Shelf Res, 30, 1275–1282, https://doi.org/10.1016/j.csr.2010.04.005, 2010.

Munkes, B., Löptien, U., and Dietze, H.: Cyanobacteria blooms in the Baltic Sea: A review of models and facts, Biogeosciences, 18, 2347–2378, https://doi.org/10.5194/bg-18-2347-2021, 2021.

Murray, C. J., Müller-Karulis, B., Carstensen, J., Conley, D. J., Gustafsson, B. G., and Andersen, J. H.: Past, present and future eutrophication status of the Baltic Sea, Front Mar Sci, 6, https://doi.org/10.3389/fmars.2019.00002, 2019.

Mustaffa, N. I. H., Ribas-Ribas, M., Banko-Kubis, H. M., and Wurl, O.: Global reduction of in situ CO2 transfer velocity by natural surfactants in the sea-surface microlayer, Proceedings of the Royal Society A: Mathematical, Physical and Engineering Sciences, 476, https://doi.org/10.1098/rspa.2019.0763, 2020.

Nausch, G.; Feistel, R.; Lass, H. U.; Nagel, K.; Siegel, H.: Hydrographisch-chemische Zustandseinschätzung der Ostsee 2001, Meereswiss. Ber. 49, 2002

https://doi.org/10.5194/egusphere-2025-5385
Preprint. Discussion started: 18 November 2025

Nürnberg, D. J., Mariscal, V., Bornikoel, J., Nieves-Morión, M., Krauß, N., Herrero, A., Maldener, I., Flores, E., and Mullineaux, C. W.: Intercellular diffusion of a fluorescent sucrose analog via the septal junctions in a filamentous cyanobacterium, mBio, 6, https://doi.org/10.1128/mBio.02109-14, 2015.

Ohlendieck, U., Stuhr, A., and Siegmund, H.: Nitrogen fixation by diazotrophic cyanobacteria in the Baltic Sea and transfer of the newly fixed nitrogen to picoplankton organisms, Journal of Marine Systems, 25, 213–219, https://doi.org/10.1016/S0924-7963(00)00016-6, 2000.

Paczkowska, J., Rowe, O. F., Schlüter, L., Legrand, C., Karlson, B., and Andersson, A.: Allochthonous matter: An important factor shaping the phytoplankton community in the Baltic Sea, J Plankton Res, 39, 23–34, https://doi.org/10.1093/plankt/fbw081, 2017.

Paerl, H. W. and Paul, V. J.: Climate change: Links to global expansion of harmful cyanobacteria, Water Res, 46, 1349–1363, https://doi.org/10.1016/j.watres.2011.08.002, 2012.

Pannard, A., Pédrono, J., Bormans, M., Briand, E., Claquin, P., and Lagadeuc, Y.: Production of exopolymers (EPS) by cyanobacteria: impact on the carbon-to-nutrient ratio of the particulate organic matter, Aquat Ecol, 50, 29–44, https://doi.org/10.1007/s10452-015-9550-3, 2016.

Parrish, C. C.: Lipid biogeochemistry of plankton, settling matter and sediments in Trinity Bay, Newfoundland. I. Lipid classes, Organic Geochemistry 29.5-7, 1531-1545, 1998.

Pereira, R., Schneider-Zapp, K., and Upstill-Goddard, R. C.: Surfactant control of gas transfer velocity along an offshore coastal transect: Results from a laboratory gas exchange tank, Biogeosciences, 13, 3981–3989, https://doi.org/10.5194/bg-13-3981-2016, 2016.

Pereira, R., Ashton, I., Sabbaghzadeh, B., Shutler, J. D., and Upstill-Goddard, R. C.: Reduced air-sea CO2 exchange in the Atlantic Ocean due to biological surfactants, Nat Geosci, 11, 492–496, https://doi.org/10.1038/s41561-018-0136-2, 2018.

De Philippis, R. and Vincenzini, M.: Exocellular polysaccharides from cyanobacteria and their possible applications, FEMS Microbiol Rev, 22, 151–175, https://doi.org/10.1111/j.1574-6976.1998.tb00365.x, 1998.

Van Pinxteren, M., Müller, C., Iinuma, Y., Stolle, C., and Herrmann, H.: Chemical characterization of dissolved organic compounds from coastal sea surface microlayers (Baltic Sea, Germany), Environ Sci Technol, 46, 10455–10462, https://doi.org/10.1021/es204492b, 2012.

Ploug, H.: Cyanobacterial surface blooms formed by Aphanizomenon sp. and Nodularia spumigena in the Baltic Sea: Small-scale fluxes, pH, and oxygen microenvironments, Limnol Oceanogr, 53, 914–921, https://doi.org/10.4319/lo.2008.53.3.0914, 2008.

Rickard, P. C., Uher, G., and Upstill-Goddard, R. C.: Photo-Reactivity of Surfactants in the Sea-Surface Microlayer and Subsurface Water of the Tyne Estuary, UK, Geophys Res Lett, 49, https://doi.org/10.1029/2021GL095469, 2022.

Sabbaghzadeh, B., Upstill-Goddard, R. C., Beale, R., Pereira, R., and Nightingale, P. D.: The Atlantic Ocean surface microlayer from 50°N to 50°S is ubiquitously enriched in surfactants at wind speeds up to 13 m s−1, Geophys Res Lett, 44, 2852–2858, https://doi.org/10.1002/2017GL072988, 2017.

https://doi.org/10.5194/egusphere-2025-5385
Preprint. Discussion started: 18 November 2025

Satpute, S. K., Banat, I. M., Dhakephalkar, P. K., Banpurkar, A. G., and Chopade, B. A.: Biosurfactants, bioemulsifiers and exopolysaccharides from marine microorganisms, https://doi.org/10.1016/j.biotechadv.2010.02.006, July 2010.

Schmidt, R. and Schneider, B.: The effect of surface films on the air-sea gas exchange in the Baltic Sea, Mar Chem, 126, 56–62, https://doi.org/10.1016/j.marchem.2011.03.007, 2011.

Scholz, F.: Voltammetric techniques of analysis: the essentials, ChemTexts, 1, https://doi.org/10.1007/s40828-015-0016-y, 2015.

Seidel, M., Manecki, M., Herlemann, D. P. R., Deutsch, B., Schulz-Bull, D., Jürgens, K., and Dittmar, T.: Composition and Transformation of Dissolved Organic Matter in the Baltic Sea, Front Earth Sci (Lausanne), Volume 5-2017, 2017.

Seppälä, J., Ylöstalo, P., Kaitala, S., Hällfors, S., Raateoja, M., and Maunula, P.: Ship-of-opportunity based phycocyanin fluorescence monitoring of the filamentous cyanobacteria bloom dynamics in the Baltic Sea, Estuar Coast Shelf Sci, 73, 489–500, https://doi.org/10.1016/J.ECSS.2007.02.015, 2007.

Sharp, J. H.: Improved analysis for “particulate” organic carbon and nitrogen from seawater, Limnology and Oceanography 19.6, 984-989, https://doi.org/10.4319/lo.1974.19.6.0984, 1974.

Śliwińska-Wilczewska, S., Felpeto, A. B., Mozdzeń, K., Vasconcelos, V., and Latała, A.: Physiological effects on coexisting microalgae of the allelochemicals produced by the bloom-forming cyanobacteria synechococcus sp. And nodularia spumigena, Toxins (Basel), 11, https://doi.org/10.3390/toxins11120712, 2019.

Sondergaard, M.: Phototrophic Picoplankton in Temperate Lakes : Seasonal Abundance and Importance along a Trophic Gradient, 1991.

Springstein, B. L., Weissenbach, J., Koch, R., Stücker, F., and Stucken, K.: The role of the cytoskeletal proteins MreB and FtsZ in multicellular cyanobacteria, FEBS Open Bio, 10, 2510–2531, https://doi.org/10.1002/2211-5463.13016, 2020.

Stal, L. J.: Microphytobenthos, their Extracellular Polymeric Substances, and the Morphogenesis of Intertidal Sediments, Geomicrobiol J, 20, 463–478, https://doi.org/10.1080/713851126, 2003.

Stal, L. J., Staal, M., and Villbrandt, M.: Nutrient control of cyanobacterial blooms in the Baltic Sea, 165–173 pp., 1999.

Stolle, C., Nagel, K., Labrenz, M., and Jürgens, K.: Succession of the sea-surface microlayer in the coastal Baltic Sea under natural and experimentally induced low-wind conditions, Biogeosciences, 7, 2975–2988, https://doi.org/10.5194/bg-7-2975-2010, 2010.

Stolle, C., Ribas-Ribas, M., Badewien, T. H., Barnes, J., Carpenter, L. J., Chance, R., Damgaard, L. R., Durán Quesada, A. M., Engel, A., Frka, S., Galgani, L., Gašparović, B., Gerriets, M., Hamizah Mustaffa, N. I., Herrmann, H., Kallajoki, L., Pereira, R., Radach, F., Revsbech, N. P., Rickard, P., Saint, A., Salter, M., Striebel, M., Triesch, N., Uher, G., Upstill-Goddard, R. C., van Pinxteren, M., Zäncker, B., Zieger, P., and Wurl, O.: The MILAN Campaign: Studying Diel Light Effects on the Air–Sea Interface, Bull Am Meteorol Soc, 101, E146–E166, https://doi.org/https://doi.org/10.1175/BAMS-D-17-0329.1, 2020.

Stråat, K. D., C. M. Mörth, A. Sobek, Smedberg, E., and Undeman, E.: Modeling total particulate organic carbon (POC) flows in the Baltic Sea catchment. Biogeochemistry, 128, 51–65, doi:10.1007/s10533-016-0194-8, 2016

https://doi.org/10.5194/egusphere-2025-5385
Preprint. Discussion started: 18 November 2025

Stuart, R. K., Mayali, X., Lee, J. Z., Craig Everroad, R., Hwang, M., Bebout, B. M., Weber, P. K., Pett-Ridge, J., and Thelen, M. P.: Cyanobacterial reuse of extracellular organic carbon in microbial mats, ISME J, 10, 1240–1251, https://doi.org/10.1038/ismej.2015.180, 2016.

Tamm, M., Laas, P., Freiberg, R., Nõges, P., and Nõges, T.: Parallel assessment of marine autotrophic picoplankton using flow cytometry and chemotaxonomy, Science of The Total Environment, 625, 185–193, https://doi.org/10.1016/J.SCITOTENV.2017.12.234, 2018.

Taylor, J. D., Cottingham, S. D., Billinge, J., and Cunliffe, M.: Seasonal microbial community dynamics correlate with phytoplankton-derived polysaccharides in surface coastal waters, ISME Journal, 8, 245–248, https://doi.org/10.1038/ismej.2013.178, 2014.

Thornton, D. C. O.: Dissolved organic matter (DOM) release by phytoplankton in the contemporary and future ocean, Eur J Phycol, 49, 20–46, https://doi.org/10.1080/09670262.2013.875596, 2014.

Thornton, D.C., Brooks, S.D. and Chen, J.: Protein and carbohydrate exopolymer particles in the sea surface microlayer (SML). Frontiers in Marine Science, 3, p.135, 2016

Thornton, D. C. O.: Coomassie Stainable Particles (CSP): Protein containing exopolymer particles in the ocean, Frontiers in Marine Science 5, 206, https://doi.org/10.3389/fmars.2018.00206, 2018.

Tomitani, A., Knoll, A. H., Cavanaugh, C. M., and Ohno, T.: The evolutionary diversification of cyanobacteria: Molecular-phylogenetic and paleontological perspectives, 2006.

Tsai, W. ting and Liu, K. K.: An assessment of the effect of sea surface surfactant on global atmosphere-ocean CO2 flux, J Geophys Res Oceans, 108, https://doi.org/10.1029/2000jc000740, 2003.

Utermöhl, H.: Zur Vervollkommnung der quantitativen Phytoplankton-Methodik, Internationale Vereinigung für Theoretische und Angewandte Limnologie: Mitteilungen, 9, 1–38, https://doi.org/10.1080/05384680.1958.11904091, 1958.

Wasmund, N.: Occurrence of cyanobacterial blooms in the baltic sea in relation to environmental conditions, Internationale Revue der Gesamten Hydrobiologie, 82, 169–184, https://doi.org/10.1002/iroh.19970820205, 1997.

Wurl, O. and Obbard, J. P.: A review of pollutants in the sea-surface microlayer (SML): a unique habitat for marine organisms, Mar Pollut Bull, 48, 1016–1030, https://doi.org/10.1016/J.MARPOLBUL.2004.03.016, 2004.

Wurl, O., and Holmes, M.: The gelatinous nature of the sea-surface microlayer. Mar. Chem. 110, 89–97. doi:10.1016/j.marchem.2008.02.009, 2008

Wurl, O., Wurl, E., Miller, L., Johnson, K., and Vagle, S.: Formation and global distribution of sea-surface microlayers, Biogeosciences, 8, 121–135, https://doi.org/10.5194/bg-8-121-2011, 2011.

Wurl, O., Stolle, C., Van Thuoc, C., The Thu, P., and Mari, X.: Biofilm-like properties of the sea surface and predicted effects on air–sea CO2 exchange, Prog Oceanogr, 144, 15–24, https://doi.org/10.1016/J.POCEAN.2016.03.002, 2016.

Wurl, O., Ekau, W., Landing, W. M., and Zappa, C. J.: Sea surface microlayer in a changing ocean - A perspective, https://doi.org/10.1525/elementa.228, 2017.

https://doi.org/10.5194/egusphere-2025-5385
Preprint. Discussion started: 18 November 2025

Wurl, O., Bird, K., Cunliffe, M., Landing, W. M., Miller, U., Mustaffa, N. I. H., Ribas-Ribas, M., Witte, C., and Zappa, C. J.: Warming and Inhibition of Salinization at the Ocean's Surface by Cyanobacteria, Geophys Res Lett, 45, 4230–4237, https://doi.org/10.1029/2018GL077946, 2018.

Zäncker, B., Bracher, A., Röttgers, R., and Engel, A.: Variations of the organic matter composition in the sea surface microlayer: A comparison between open ocean, coastal, and upwelling sites off the Peruvian coast, Front Microbiol, 8, https://doi.org/10.3389/fmicb.2017.02369, 2017.

Zettler, M. L., Kremp, A., and Dutz, J.: Biological assessment of the Baltic Sea 2022, https://doi.org/10.12754/msr-2024-0125, 2024.

Zhang, Z., Liu, L., Liu, C., and Cai, W.: Studies on the sea surface microlayer: II. The layer of sudden change of physical and chemical properties, J Colloid Interface Sci, 264, 148–159, https://doi.org/10.1016/S0021-9797(03)00390-4, 2003.

Zhi, W., Klingler, C., Liu, J., and Li, L.: Widespread deoxygenation in warming rivers, Nat Clim Chang, 13, 1105–1113, https://doi.org/10.1038/s41558-023-01793-3, 2023.

Zufia, J. A., Farnelid, H., and Legrand, C.: Seasonality of Coastal Picophytoplankton Growth, Nutrient Limitation, and Biomass Contribution, Front Microbiol, 12, https://doi.org/10.3389/fmicb.2021.786590, 2021.

Zutic, V., Cosovic, B., and Bihari, N.: Surfactant production by marine phytoplankton, Marine Chemistry, 505–520 pp., 1981.